Journal of Medicinal Chemistry

Article

pubs.acs.org/jmc

Discovery of the First Thumb Pocket 1 NS5B Polymerase Inhibitor (BILB 1941) with Demonstrated Antiviral Activity in Patients Chronically Infected with Genotype 1 Hepatitis C Virus (HCV)

Pierre L. Beaulieu,* Michael Bös, Michael G. Cordingley, Catherine Chabot, Gulrez Fazal, Michel Garneau, James R. Gillard, Eric Jolicoeur, Steven LaPlante, Ginette McKercher, Martin Poirier, Marc-André Poupart, Youla S. Tsantrizos, Jianmin Duan, and George Kukolj

Research and Development, Boehringer Ingelheim (Canada) Ltd., 2100 Cunard Street, Laval, Quebec, H7S 2G5, Canada

Supporting Information

ABSTRACT: Combinations of direct acting antivirals (DAAs) that have the potential to suppress emergence of resistant virus and that can be used in interferon-sparing regimens represent a preferred option for the treatment of chronic HCV infection. We have discovered allosteric (thumb pocket 1) non-nucleoside inhibitors of HCV NS5B polymerase that inhibit replication in replicon systems. Herein, we report the late-stage optimization of indole-based inhibitors, which began with the identification of a metabolic liability common to many previously reported inhibitors in this series. By use of parallel synthesis techniques, a sparse matrix of inhibitors was generated that provided a collection of inhibitors satisfying potency criteria and displaying improved in vitro ADME profiles. "Cassette" screening for oral absorption in rat provided a short list of potential development candidates. Further evaluation led to the discovery of the first thumb pocket 1 NS5B inhibitor (BILB 1941) that demonstrated antiviral activity in patients chronically infected with genotype 1 HCV.

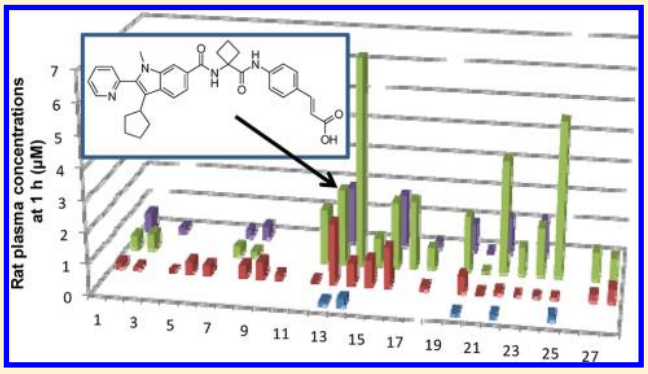

INTRODUCTION

Hepatitis C virus (HCV) was identified as the ethological agent of non-A/non-B hepatitis in 1989, and current worldwide prevalence of chronic carriers is estimated at 130−170 million people (2−3% of the world population; 5 million in the U.S.).[1,2] HCV is classified in the hepacivirus genus of the flaviviridae family, and six major genotypes have been characterized in addition to minor variants and a swarm of quasi-species resulting from error-prone replication.[3] While the origins of HCV remain unknown, the virus is mostly transmitted through contaminated blood products (e.g., blood transfusions), unsafe medical procedures, and practices among intravenous drug users. Following an acute HCV infection, most individuals will progress to a chronic state and are at risk of developing over time (20−30 years) serious and often fatal liver diseases such as cirrhosis (20%) and hepatocellular carcinomas (2%). Although the incidence of transmission has decreased dramatically, projected mortality from such conditions will increase over the next 20 years as a result of the long incubation period. Rates of HCV-related hepatocellular carcinomas (HCC) and HCV-related mortalities are projected to triple by 2030.[4] An estimated 86 000 death/year can be linked to conditions resulting from HCV infection.[5] HCV is also the leading cause for liver transplantation in industrialized nations, imposing a significant economic burden on health care systems. Furthermore, such procedures only provide temporary reprieve, as in most cases the transplanted organ becomes reinfected within a year or 2.

Until recently, HCV therapy relied on the patient's ability to mount an immune response against the virus and consisted of a combination of pegylated interferon-α (PegIFN) and ribavirin (RBV), a broad-spectrum antiviral agent. Genotype 1a/1b, which predominates in North America, Europe, and Japan, is most refractory to treatment. With this regimen sustained viral responses (SVRs), a good predictor of cure, rarely exceed 50%.[6] Furthermore, PegIFN/RBV therapy is associated with severe limiting side effects that lead to significant treatment discontinuations and contraindications that prevent use in 15% of patients.[7] In the 20 years following the initial discovery of the virus, HCV research has evolved at an unprecedented pace in both academic and industrial laboratories, providing a detailed understanding of the virus life cycle and tools to support drug discovery activities. Most notably, the development of the cell-based replicon system that supports HCV subgenomic RNA replication and the discovery of infectious virus that allows replication of the pathogen in a laboratory environment contributed greatly to this effort.[8−10] The 9.6 kb

Received: May 15, 2012
Published: July 31, 2012

dx.doi.org/10.1021/jm3006788 | J. Med. Chem. 2012, 55, 7650−7666

single (+)-strand RNA HCV genome encodes both structural and nonstructural (NS2 → NS5) proteins whose functions within a replication complex are essential for viral replication and/or infection.[11] The NS3/4A protease became one of the initial focuses of drug discovery efforts. Structure-based peptidomimetic strategies soon yielded encouraging results when Boehringer Ingelheim's celuprivir became the first small molecule drug to demonstrate potent antiviral activity in HCV-infected patients and validated available HCV research tools.[12] This milestone was followed by the recent approval in mid-2011 of the first direct acting antiviral (DAA) agents that target NS3/4A. Specifically, two first generation protease inhibitors (boceprevir from Merck and telaprevir from Vertex Pharmaceuticals) have been approved for use in combination with PegIFN/RBV.[13] Despite improved outcome, these regimens still suffer from the combined side effects of both the PegIFN/RBV-based standard of care (SoC) and the new drugs themselves. In addition, the reduced effectiveness among treatment-experienced and nonresponders to IFN-based therapies and the emergence of virus resistant to the drugs have become significant issues and represent an added layer of complexity for the development of future treatments.[14] Within the next 2 years, second generation protease inhibitors currently in phase 3 clinical trials in combination with SoC are being explored for more convenient dosing regimens and may have the potential to improve treatment options. These include Boehringer Ingelheim's faldaprevir and (2*R*,3a*R*,10-*Z*,11a*S*,12a*R*,14a*R*)-*N*-(cyclopropylsulfonyl)-2,3,3a,4,5,6,7,8,9,11a,12,13,14,14a-tetradecahydro-2-[[7-methoxy-8-methyl-2-[4-(1-methylethyl)-2-thiazolyl]-4-quinolinyl]-oxy]-5-methyl-4,14-dioxocyclopenta[*c*]cyclopropa[g][1,6]-diazacyclotetradecine-12a(1*H*)-carboxamide (TMC435350) from Tibotec.[15] Most significant, however, is the recent paradigm shift toward the development of interferon-sparing therapies using combination of DAAs with complementary modes-of-action (e.g., protease + NS5B polymerase inhibitors or NS5A ligands as well as nucleoside NS5B + NS5A combinations), which are expected to provide efficacy with improved safety and tolerability while minimizing emergence of resistant virus.[16]

By extension of precedent from successful anti-HIV strategies, the HCV NS5B RNA-dependent RNA polymerase (RdRp) target rapidly attracted considerable attention from drug designers. The 65 kDa protein, located at the C-terminal of the HCV-translated polyprotein, plays a central role in the replication of the HCV RNA genome.[17] The NS5B catalytic machinery has no close mammalian counterpart, making it an attractive target for drug intervention. It functions inside the cell as a component of the HCV replicase complex. The enzyme shares the common folds of other nucleic acid polymerases with characteristic thumb, finger, and palm domains (Figure 1).[18] NS5B has revealed itself as the most druggable HCV protein, as reflected by the publication of greater than 400 patent applications covering small molecule inhibitors of this enzyme in the past 15 years.[19] Not surprisingly, nucleoside analogues (particularly chain-terminating 2′-*C*-methyl nucleosides) were soon reported to specifically inhibit enzyme activity, and this class of active site directed inhibitors was soon validated in the clinic.[20] Today, nucleoside NS5B inhibitors continue to provide encouraging results, either in combination with SoC or with complementary DAAs, because of the conserved nature of the nucleotide binding site, high barrier to resistance, and their pan-genotype activity.[14a,21]

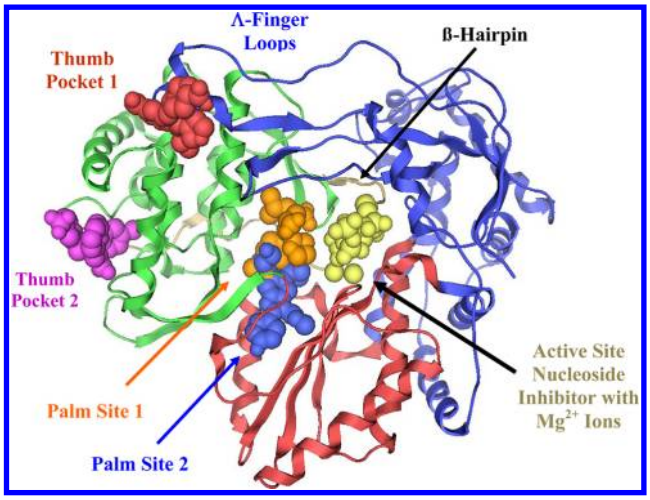

Figure 1. Three dimensional structure of NS5B with inhibitor binding sites. The three-dimensional structure of NS5B is shown in ribbon representation with the palm domain colored in red, the thumb domain in green and the finger domain with the Λ finger loops in blue. Inhibitor binding sites are depicted using CPK models of representative inhibitors: thumb pocket 1 (acetamideindolecarboxylic acid, red), thumb pocket 2 (phenylalanine derivative, magenta), palm site 1 (acylpyrrolidine, orange), palm site 2 (benzofuran derivative, blue), active site (nucleoside analog with two Mg^{2+} ions, yellow). Reproduced with permission from *Expert Opinion on Therapeutic Patents*.[19a] Copyright 2009 Informa Healthcare.

A parallel effort to nucleoside-based inhibitors began in the late 1990s, when several companies began interrogating their corporate collection for small molecule inhibitors of NS5B activity. During the subsequent years, at least four allosteric sites were uncovered that regulate enzyme function by interfering with conformational changes required during RNA synthesis. Indeed, HCV polymerase is characterized by a *β*-hairpin loop protruding in the central RNA-binding channel of the enzyme and two additional loops (Λ1 and Λ2) that extend from the fingers to the northern surface of the thumb domain, all of which are thought to be involved in the regulation of RNA synthesis, thus providing opportunities for interfering with enzymatic activity using small molecules (Figure 1).[17c,18,22]

The location of NS5B allosteric binding sites is depicted in Figure 1, with representative inhibitors bound in their pockets.[19a] Two allosteric sites are located in the thumb domain (thumb pockets 1and 2), while two others are located in the palm region (palm sites 1 and 2) near the base of the thumb domain and proximal to the enzyme active site. Binding to any of these allosteric sites blocks initiation of processive RNA synthesis by interfering with protein conformational changes, thus blocking viral replication. Binding of small molecules to these allosteric sites is usually inferred from selection of resistant genomes using the cell-based replicon system and in many cases confirmed with X-ray structural data. Clinical proof of concept in HCV-infected patients has been reported for inhibitors (see Figure 2 for example of published representative NS5B inhibitors currently in clinical development) that bind to any of the four allosteric binding sites.[19a,c,23]

Over the past years, we and others have been reporting on the discovery and optimization of benzimidazole derivatives that bind to NS5B thumb pocket 1 and block viral replication by interfering with the interaction of the Λ1 finger loop with the northern portion of the thumb domain, preventing

dx.doi.org/10.1021/jm3006788 | *J. Med. Chem.* 2012, 55, 7650−7666

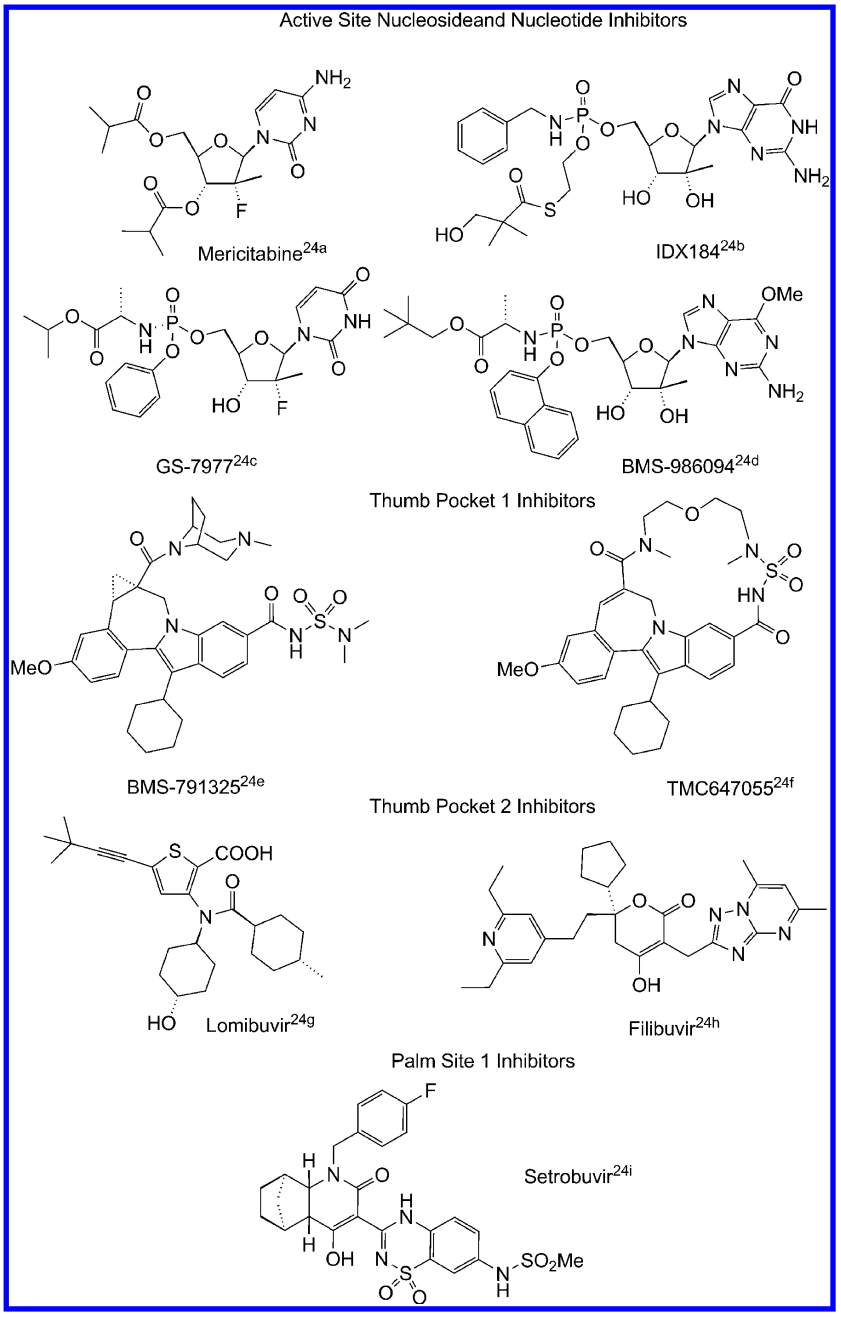

Figure 2. Structure of published representative NS5B inhibitors currently in clinical development.[24]

formation of a productive conformation that is necessary for the initiation of viral RNA synthesis. This class of inhibitors, which we refer to as "finger loop inhibitors", was initially discovered in a high-throughput screening campaign (compound **1**, Figure 3).[25] Specific and potent inhibitors of NS5B enzymatic activity were rapidly discovered, but benzimidazoles such as **2** lacked activity in cell-based assays because of the poor permeability associated with the highly ionized structures.[26] Screening for replacements of the highly polar amino acid derived right-hand side led to the discovery of diamide derivatives with comparable intrinsic biochemical potency and weak cell-based replicon activity (e.g., **3**),[27] providing a cellular proof of concept for the mechanism by which these inhibitors interfere with HCV replication. Replacement of the benzimidazole core by a more lipophilic indole scaffold provided derivatives such as **4**, with improved cell permeability and promising efficacy in the subgenomic replicon system. While inhibitors such as **4** achieved a cell-based potency target (replicon gt1 EC_{50} < 100 nM) for further progression, they generally lacked the necessary ADME-PK attributes (e.g., metabolic stability) for selection as development candidates.[28]

Herein, we report on the late stage optimization of this class of inhibitors. This effort began with the identification of a metabolic liability common to many previously reported inhibitors in this series (e.g., compound **4**) followed by replacement of the metabolic "hot spot" and the generation of compound matrices combining diverse beneficial structural features at the indole C2 position and the right-hand side of the molecules to identify analogues with optimized properties. This effort, which made extensive use of our parallel synthesis capabilities, provided a collection of molecules that fulfilled potency and selectivity criteria. Following further profiling,

dx.doi.org/10.1021/jm3006788 | J. Med. Chem. 2012, 55, 7650−7666

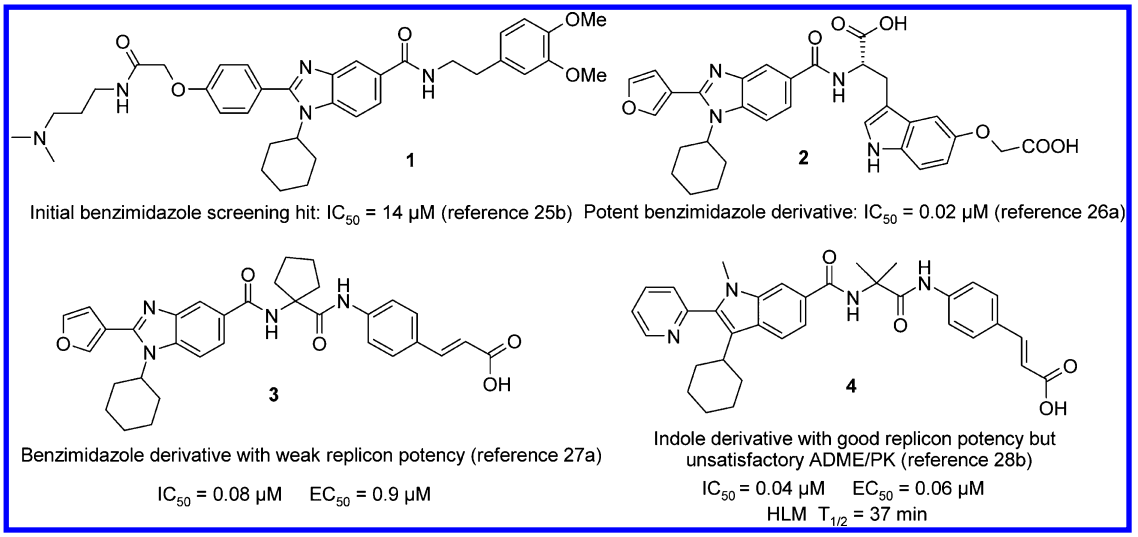

Figure 3. SAR progression of benzimidazole thumb pocket 1 HCV NS5B inhibitors.

Scheme 1. Major Metabolic Pathway and MS/MS Fragmentation Pattern for Compound 4

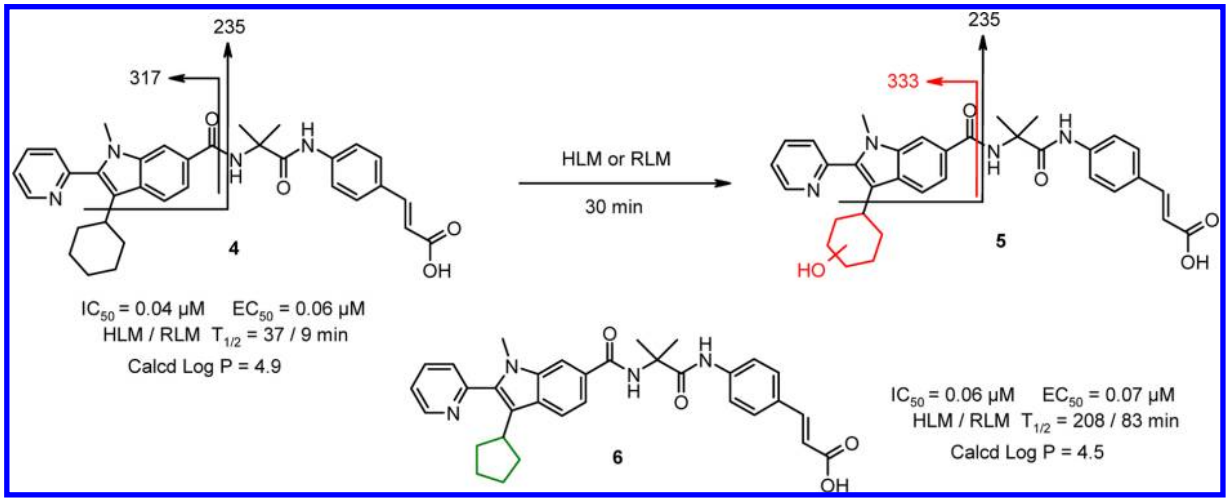

molecules with satisfactory in vitro ADME characteristics (particularly metabolic stability and Caco-2 permeability) were screened in "cassette mode" for oral absorption in rat, providing a short list of potential development candidates. Further evaluation led to the identification of **D13**, the first thumb pocket 1 HCV NS5B clinical candidate to demonstrate efficacy in genotype 1 HCV-infected patients.[29]

RESULTS AND DISCUSSION

In recent publications,[28a,b] we described a series of indole diamide derivatives (e.g., compound **4**) that in cell culture experiments inhibited replication of gt1-HCV subgenomic replicons with EC_{50} < 100 nM. However, the majority of compounds in this class exhibited high lipophilicity (calculated log P > 5) with poor aqueous solubility at physiological pH, low metabolic stability in the presence of liver microsome preparations ($T_{1/2}$ < 60 min), and high in vivo clearance in rat. Attempts to reduce lipophilicity by introducing polar features onto the molecule while improving metabolic stability in some cases generally resulted in reduced Caco-2 permeability, and lack of oral exposure in rat and/or significantly reduced antiviral potency in cell-based assays. In order to identify candidates for advancement into clinical development, we therefore envisaged a stepwise strategy whereby the ADME-PK profile of this class would be improved through identification of metabolic liabilities (hot spots) followed by conservative modifications to address these liabilities while minimizing the impact on other parameters (e.g., potency and Caco-2 permeability). To this end, compound **4** was incubated with human and rat liver microsome preparations. In each case, a single major metabolite **5** was detected (indistinguishable by HPLC and MS fragmentation pattern for both species) resulting from hydroxylation of the 3-cyclohexyl ring at an unknown position (lack of further fragmentation precluded further localization of the oxidation site by LC−MS/MS (Scheme 1).

The identification of the cyclohexyl ring as a metabolic hot spot for this class of compound initially presented itself as a significant issue, as early SAR in benzimidazole analogues had shown this position to be extremely sensitive to structural modifications.[25b] Indeed, only replacement with cyclopentyl was tolerated, albeit with a 3-fold loss in enzymatic potency. We were therefore encouraged when in the more advanced indole series, the small change in lipophilicity resulting from replacement of the 3-cyclohexyl ring in compound **4** by a cyclopentyl moiety (compound **6**; calculated log P of 4.9 and

dx.doi.org/10.1021/jm3006788 | J. Med. Chem. 2012, 55, 7650−7666

Scheme 2. Strategy for the Identification of Potent NS5B Inhibitors with Improved ADME-PK Profiles

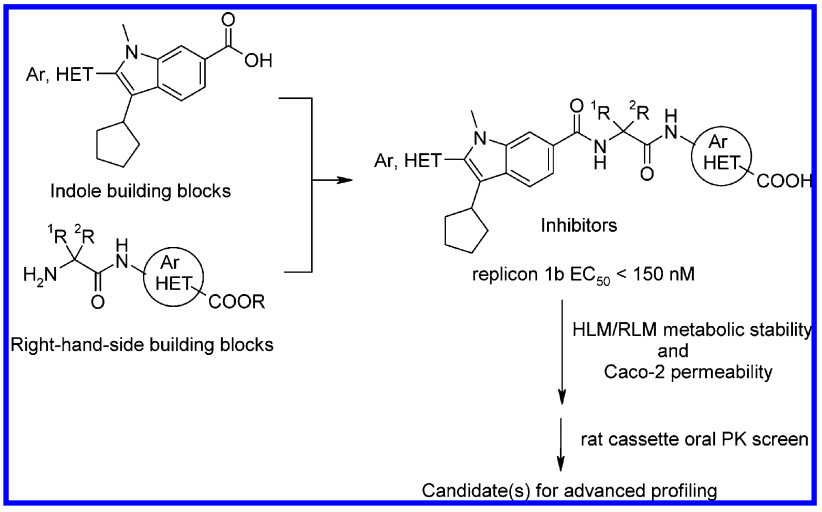

Chart 1. 3-Cyclopentyl-1-methyl-6-indolecarboxylic Acid Building Blocks

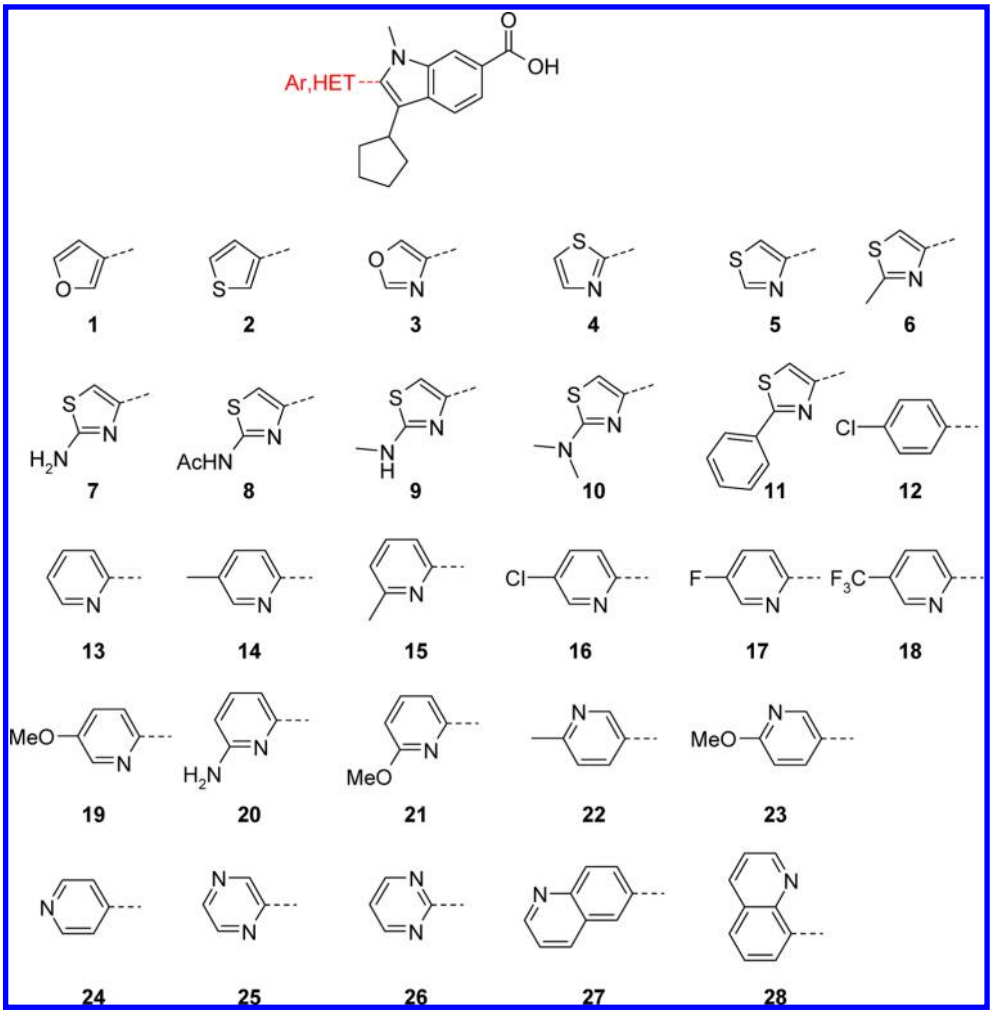

4.5 for **4** and **6**, respectively) resulted in a compound with comparable intrinsic and cell-based potency and considerably improved metabolic stability (HLM $T_{1/2}$ from 37 to 208 min). Additional metabolite identification studies performed on related analogues revealed that 3-cyclopentylindole derivatives were generally more resistant to phase 1 oxidative metabolism than the corresponding 3-cyclohexyl analogues and potency was usually maintained (results not shown). Our next objective was to apply SAR learnings from the cyclohexylindole series[28a,b] to the 3-cyclopentyl version, with the aim to identify a collection of inhibitors with improved potency (EC_{50} < 100 nM) and ADME-PK profiles for advancement into development. In order to accelerate the discovery of such inhibitors, this study was performed using high-throughput synthesis and

dx.doi.org/10.1021/jm3006788 | J. Med. Chem. 2012, 55, 7650−7666

Chart 2. Right-Hand-Side Building Blocks for Inhibitor Synthesis

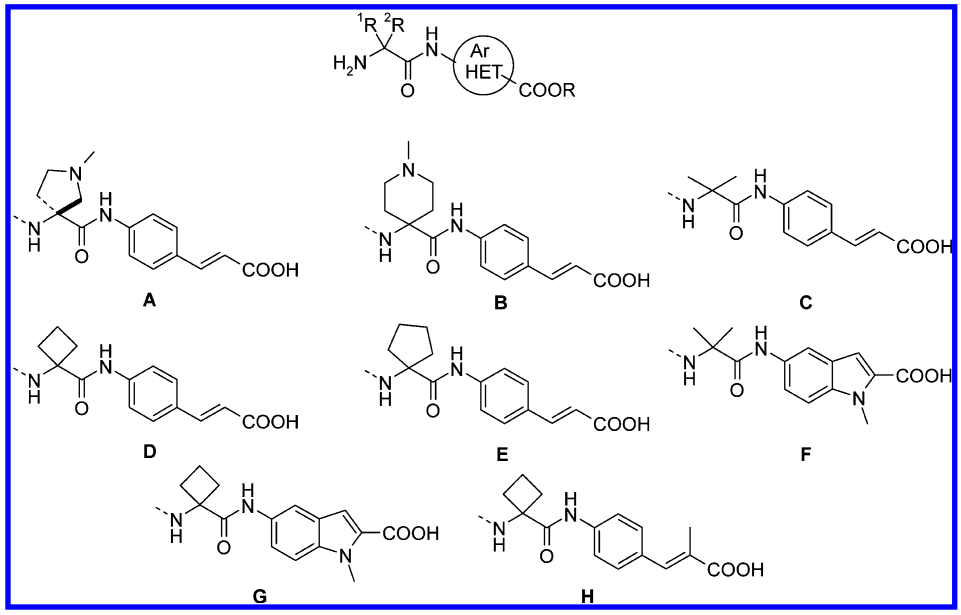

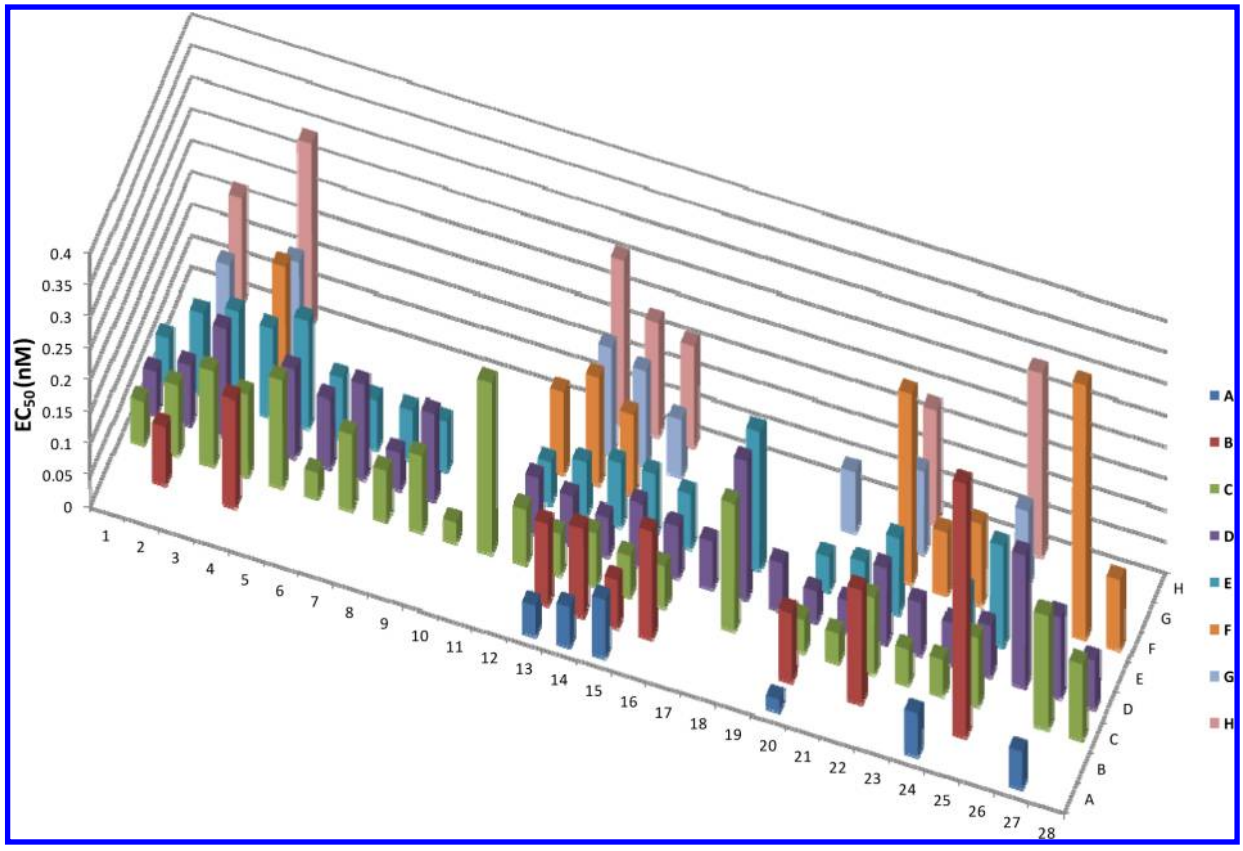

Figure 4. Replicon 1b potency for a sparse matrix of 110 representative inhibitors. C2 substituents are represented on the *X*-axis (see Chart 1 for structures) and are numbered 1−28. Right-hand sides are listed on the *Z*-axis and are labeled A− H (see Chart 2 for structures). Genotype 1b replicon potency is displayed on the *y*-axis in nM.

profiling techniques as outlined in the decision tree shown in Scheme 2.

On the basis of previously established SAR, 3-cyclopentyl-1-methyl-6-indolecarboxylic acid with various C2 substituents (Chart 1) and right-hand-side building blocks (Chart 2) were prepared independently and coupled together to provide compounds for testing (see section Chemistry for details).

Upon initial evaluation of a few inhibitors, it became apparent that SAR was directly transferable from the 3-cyclohexylindole series[28a,b] to the corresponding 3-cyclopentyl analogues. Consequently, our strategy for the rapid generation and identification of the most interesting analogues relied on the generation of a sparse matrix of 110 inhibitors using some of the more fruitful previously identified C2-substituted indole

dx.doi.org/10.1021/jm3006788 | *J. Med. Chem.* 2012, 55, 7650−7666

Table 1. Profile of Most Promising Inhibitors

	1b IC_{50} [a] (nM)	1b EC_{50} [a] (nM)	HLM $T_{1/2}$ (min)	RLM $T_{1/2}$ (min)	Caco-2 (cm/s)[b]	solubility[c] (μg/mL)	calcd log P [d]	CYP450 2C19/3A4 IC_{50} (μM)	plasma $C_{1\ h}$ [e] (μM)
A20	19	20	>300		2.9×10^{-6}	21	0.8		0.03
C13	60	67	208	83	6.5×10^{-6}	92	4.5	3.3/7.9	1.9
C16	71	67	236		1.8×10^{-6}	25	5.8	1.4/9.4	1.3
D1	69	67	162		7.5×10^{-6}	6	5.6	3.0/9.2	0.45
D12	690	89	>300	>300		0.1	7.0	2.7/8.3	1.7
D13	60	84	85	31	11.2×10^{-6}	28	4.5	2.9/9.5	2.4
D14	84	62	53	24	6.9×10^{-6}	6	4.7	0.4/5.8	6.7
D16	92	83	>300	>300		3	5.8	1.0/10.9	2.1
D17	39	76	167			8	5.5	0.8/6.7	2.2
D20	73	48	>300	62	1.8×10^{-6}	21	2.9	>30/7.0	1.8
D23	200	82	95	61	1.5×10^{-6}	0.6	5.4	0.3/1.5	0.9
D24	130	67	112	69	2.9×10^{-6}	7	3.9		1.6
D25	49	94	96	56	10×10^{-6}	49	4.2	5.1/10.6	5.0
E13	45	84	96	19	12.6×10^{-6}	16	4.9	0.9/6.3	1.9
E16	98	85	>300			4	6.2	4.3/10.7	1.7
E24	66	71	107		0.8×10^{-6}	11	4.3	2.2/4.3	1.2

[a]Values are an average of at least two determinations. [b]The Caco-2 permeability assay was run without BSA with both chambers at pH 7.4. [c]Measured on lyophilized, amorphous solids using the 24 h shaking flask method and pH 7.2 phosphate buffer. [d]JChem 5.0.0 (http://www.chemaxon.com). [e]Following oral administration to rats as mixtures of four compounds. Measured plasma concentrations were normalized to a dose of 3 mg/kg.

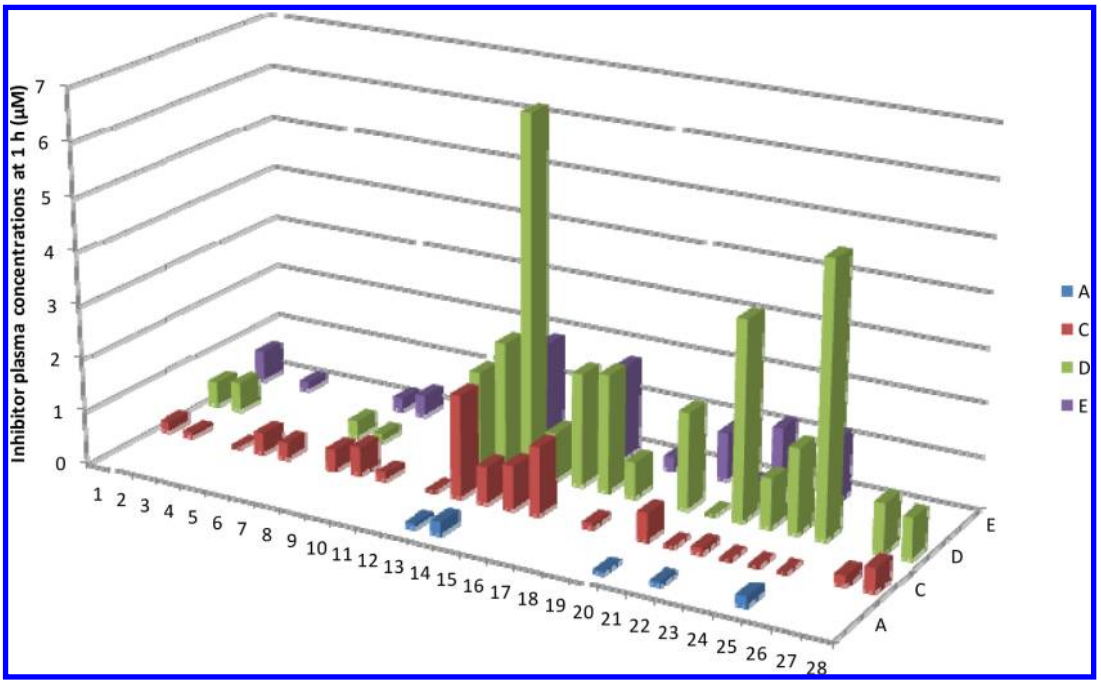

Figure 5. Inhibitor plasma concentrations (normalized to a 3 mg/kg dose) following oral dosing in rat as mixtures of 4 compounds. *X*- and *Z*-axis are labeled as in Figure 4. Inhibitor plasma concentrations (μM units) at 1 h after oral dosing are displayed on the *Y*-axis.

and right-hand-side building blocks rather than a full 190 analogue combination matrix of 28 C2 substituents and 8 right-hand-side fragments (as described in Charts 1 and 2). Nevertheless, representative compounds were prepared from all possible series in order to ensure that all potentially interesting compounds would be profiled. Replicon gt1b potency for this sparse matrix is depicted in graphical format in Figure 4, while potencies for all individual compounds are provided in the Supporting Information and data for key inhibitors are presented in Table 1. EC_{50} values in the gt1b replicon ranged from 20 to 550 nM, with (*S*)-cucurbitine **A** and alkyl/cycloalkyl **C**, **D**, and **E** cinnamic acid right-hand sides consistently providing the most potent analogues. SAR trends at C2 were less apparent, and potent analogues (EC_{50} < 100 nM) were identified for most of the 28 indole building blocks except for **3**–**5**, **11**, **18**, **22**, **25**, and **26**. As seen in previous studies,[28a,b] 3-furyl (building block **1**), substituted 2-pyridyl (building blocks **13**–**17**, **19**–**21**), 4-pyridyl (building block **24**), and some aminothiazolyl (building blocks **8**, **10**) C2 substituents provided some of the most potent analogues. In total, 49 inhibitors had $EC_{50} \leq 100$ nM (35 had EC_{50} of 100–150 nM).

Analogues with cell-based replicon potency EC_{50} < 150 nM (84 analogues; see Figure 4) were subsequently evaluated in

dx.doi.org/10.1021/jm3006788 | J. Med. Chem. 2012, 55, 7650–7666

Table 2. Single Compound Rat PK Parameters

	oral parameter (10 mg/kg)[a]			iv parameter (2 mg/kg)[b]			
	C_{max} (μM)	AUC (μM·h)	MRT (h)	V_{ss} (L/kg)	CL (mL kg^{-1} min^{-1})	$T_{1/2}$ (h)	F (%)
C13	6.4	7.2	1.7	1.3	18.2	1.7	46
D13	7.5	22.7	4.1	0.48	8.3	1.5	59
D20	3.7	8.4	3.4				
D25	7.8	17.7	2.4	0.58	6.8	2.2	41

[a]Compound dosed as an oral suspension in 0.5% Methocel and 0.3% Tween-80. [b]Bolus injection prepared in 70% PEG-400.

human and rat liver microsome (HLM/RLM) stability assays and Caco-2 permeability. From this initial profiling, 71 compounds were selected for in vivo profiling in rat. This evaluation was mostly performed using a four-compound "cassette format", whereby a mixture of four compounds was orally administered to animals at a dose of 3 or 4 mg/kg each. Inhibitor plasma concentrations were determined at 1 h after oral dosing and are reported in graphical format in Figure 5 (for comparison purposes, all 4 mg/kg data were normalized to 3 mg/kg and the individual compound data are provided in the Supporting Information). This po dosing method provided a rapid estimate of plasma exposure and provided a short list of 16 potential candidates for further profiling and prioritization (Table 1).

Figure 5 clearly shows that, except for a few derivatives (compounds **C13**–**16**), inhibitors containing the basic cucurbitine fragment or an α,α-dimethylamino acid linker (**A** and **C** right-hand sides, respectively) had significantly lower plasma levels than inhibitors containing the 1-aminocyclobutane or 1-aminocyclopentane carboxylic acid fragments (series **D** and **E**). Cyclobutane derivatives (right-hand side of **D**) were particularly well absorbed compared to other series, irrespective of the C2 substituent on the indole scaffold. In terms of individual C2 indole substituents, basic 2-, 3-, and 4-pyridyl and 2-pyridazinyl analogues provided the best plasma exposures, likely because of improved aqueous solubility at low pH. Compounds with the most promising overall profile, based on replicon potency (EC_{50} < 100 nM), metabolic stability, Caco-2 permeability, and plasma exposure in rat, are depicted in Table 1.

The most potent compound identified through this work was cucurbitine analogue **A20** with EC_{50} = 20 nM. Unfortunately, this compound did not achieve high plasma levels following rat po cassette dosing (also tested in a single rat PK experiment where C_{max} = 0.09 μM was obtained at 10 mg/kg; data not shown) and was not pursued further. Four compounds exhibiting submicromolar inhibition of CYP2C19 (also CYP2C9 for **D23**, data not shown) were also eliminated from further consideration, including **D14**, which had exhibited the highest plasma exposures in the oral cassette PK screen in rats. Compounds with low aqueous solubility at pH 7.2 (<10 μg/mL) were also deprioritized. The four remaining inhibitors were further profiled in single compound rat PK at an oral dose of 10 mg/kg administered as a suspension (see Experimental Section for details). Oral and iv parameters are presented in Table 2.

Inhibitors **D13** and **D25** (Figure 6), which have comparable replicon potency (EC_{50} of 84 and 94 nM, respectively), were identified as the most promising compounds based on plasma exposures and lower iv clearance compared to **C13** and **D20** and were advanced into higher species PK profiling in dog and rhesus monkey. The data for the two compounds are shown in Table 3.

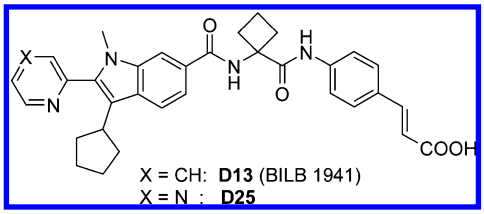

Figure 6. Structure of **D13** (BILB 1941) and **D25**.

As can be seen from Table 3, **D13** had a superior dog PK profile with higher plasma exposure and lower clearance than **D25**. **D13** also had a good PK profile when administered to rhesus monkeys.

Overall, **D13** (Figure 6) displayed a very consistent cross-species PK profile. Furthermore, a favorable partitioning of the compound between the plasma compartment and the target liver organ was observed in rat (~9-fold). On the basis of its replicon potency (gt1b/1a EC_{50} = 84/153 nM), low serum shift (~3-fold), and favorable ADME-PK characteristics, **D13** was advanced into preclinical development and eventually a proof-of-concept clinical trial in gt1 HCV-infected patients.[29]

CHEMISTRY

C2-substituted 3-cyclopentylindole-6-carboxylic acid building blocks shown in Chart 1 were synthesized in a similar fashion to the corresponding 3-cyclohexyl analogues by one of three methods (A–C) described in Scheme 3.[30] Commercially available indole-6-carboxylic acid **7** was condensed with cyclopentanone under basic conditions to provide cyclopentene **8** which was hydrogenated to cyclopentyl intermediate **9** and dimethylated to provide ester **10**. Intermediates **8** and **9** were processed as crude materials, and purification of **10** from carried-over impurities (mostly an indole dimer **11**) was accomplished by trituration. Bromination at C2 using elemental bromine provided key intermediate **12**. Introduction of the C2 indole substituent was accomplished using one of three cross-coupling methodologies depending on the availability of reagents and scale. For commercially available boronic acids, direct Suzuki–Miyaura cross-coupling to generate building blocks **1**, **2**, **12**, **15**, **27**, and **28** (Chart 1) was generally preferred (method A). Alternatively, in cases where the boronic acid was not available or chemically unstable (e.g., 2-pyridyl derivatives), bromide **12** was converted by metal–halogen exchange to tributylstannyl derivative **13** that was isolated in good yield and purity after flash chromatography using triethylamine-deactivated silica gel (stannane **13** is protolytically unstable). Intermediate **13** underwent Stille cross-coupling with a variety of aryl and heteroaryl bromides to provide C2-substituted indole building blocks **4**, **5**, **13**, **14**, **18**, **19**, **22**, and **25** in good yield (method B). Method C was used for similar cases as method B and particularly useful on larger scale to avoid inconveniences associated with the use of large quantities

Table 3. Dog and Rhesus Monkey PK Profiles for D13 and D25

	oral parameter (10 mg/kg)[a]			iv parameter (2 mg/kg)[b]			
	C_{max} (μM)	AUC (μM·h)	MRT (h)	V_{ss} (L/kg)	CL (mL kg^{-1} min^{-1})	$T_{1/2}$ (h)	F (%)
D13 (dog)	15.3	99	5.4	0.54	1.8	4.3	64
D25 (dog)	10.9	37.4	3.9	0.75	4.3	1.6	54
D13 (monkey)	6.4	20.5	2.9	0.70	9.5	1.7	70

[a]Compound dosed as an oral suspension in 0.5% Methocel and 0.3% Tween-80. [b]Bolus injection prepared in 70% PEG-400.

Scheme 3. Synthesis of C2-Substituted 3-Cyclopentyl-6-indolecarboxylic Acids[a]

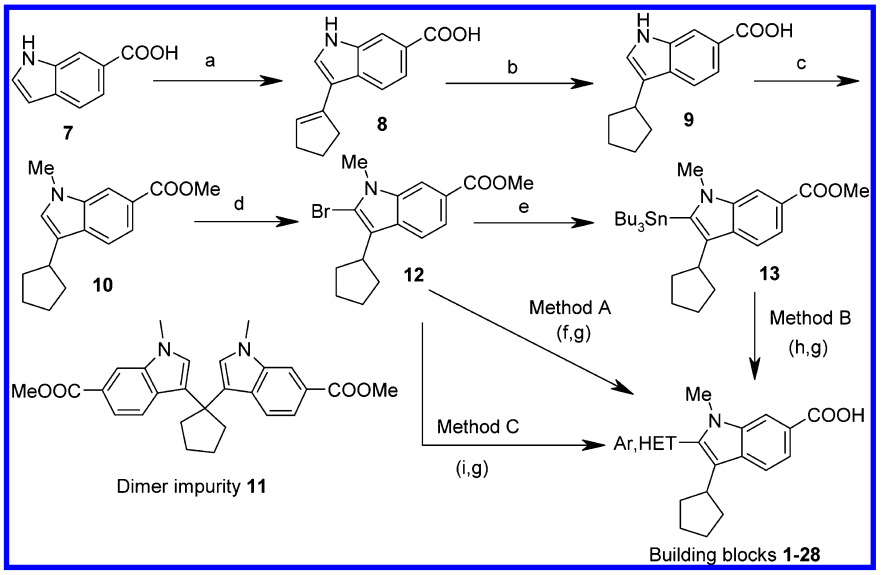

[a](a) cyclopentanone, KOH, MeOH–water, 75 °C; (b) 20% $Pd(OH)_2$/C, MeOH, H_2 (1 atm); (c) K_2CO_3, MeI, DMF, rt then NaH, MeI, 0 °C to rt; (d) NaOAc, Br_2, *i*-PrOAc, 4 °C; (e) *n*-BuLi, Bu_3SnCl, THF, −72 °C to rt. Method A: heteroaryl- or arylboronic acid (1.3 equiv), LiCl (2 equiv), Na_2CO_3 (2.5 equiv), $Pd(PPh_3)_4$ (0.04 equiv), degassed toluene/ethanol/water 1:1:1, reflux overnight under argon; (g) NaOH, THF–MeOH. (h) Method B: heterocycle bromide, $Pd(Ph_3P)_4$, CuI, LiI, $P(Ph)_3$, DMF, 100 °C. (i) Method C: *n*-BuLi, $B(OMe)_3$, THF, −71 °C to rt, then $Pd(OAc)_2$, $P(p\text{-tolyl})_3$, K_2CO_3, heterocycle bromide, MeOH, reflux.

Scheme 4. Synthesis of Substituted Thiazolylindole Building Blocks Using the Hantzsch Synthesis (7–11)[a]

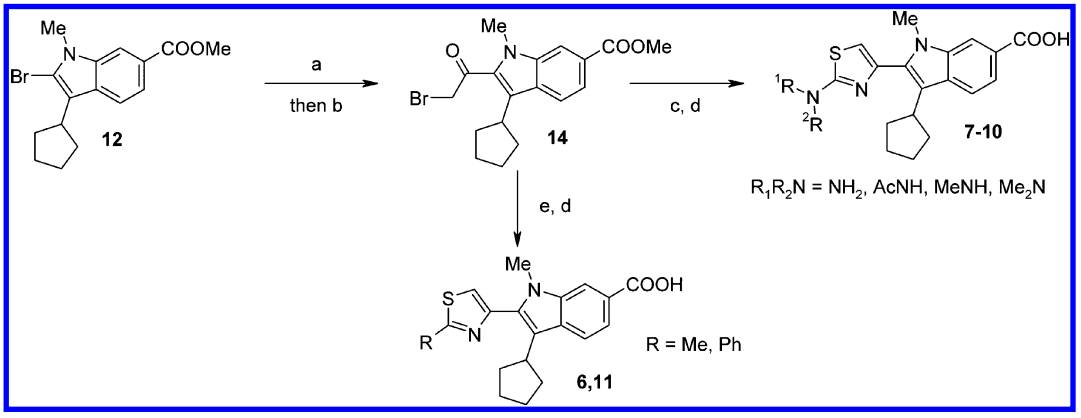

[a](a) 1-ethoxytributylvinylstannane, $PdCl_2(PPh_3)_2$, dioxane, 100 °C; (b) *N*-bromosuccinimide, THF–water, 0 °C; (c) thiourea, *i*-PrOH or dioxane, 80–100 °C; (d) LiOH, THF–MeOH–water; (e) thioamide, dioxane, 80 °C.

of tin derivatives. In this case, bromide **12** was converted to a boronate ester through a metal–halogen exchange and cross-coupled in situ to halides using Suzuki–Miyaura conditions. Building blocks **4**, **13**, **16**, **17**, **20**, **21**, **23**, and **24–26** were prepared in this fashion.

The synthesis of substituted thiazole building blocks is depicted in Scheme 4 and makes use of the Hantzsch thiazole synthetic protocol.[31] Bromide **12** was converted to bromoketone **14** by Stille cross-coupling with 1-ethoxytributylvinylstannane followed by bromination under protic conditions. Thiazole-containing building blocks **6–11** (Chart 1 and others not shown) were then accessed by reaction with various thioamides and thioureas.

The synthesis of inhibitors containing a (*S*)-cucurbitine right-hand side **A** is detailed in Scheme 5. The amino functions of (*S*)-(−)-cucurbitine **15**[32] were differentially protected as the

dx.doi.org/10.1021/jm3006788 | *J. Med. Chem.* 2012, 55, 7650–7666

Scheme 5. Synthesis of (*S*)-Cucurbitine Right-Hand-Side Fragment A[a]

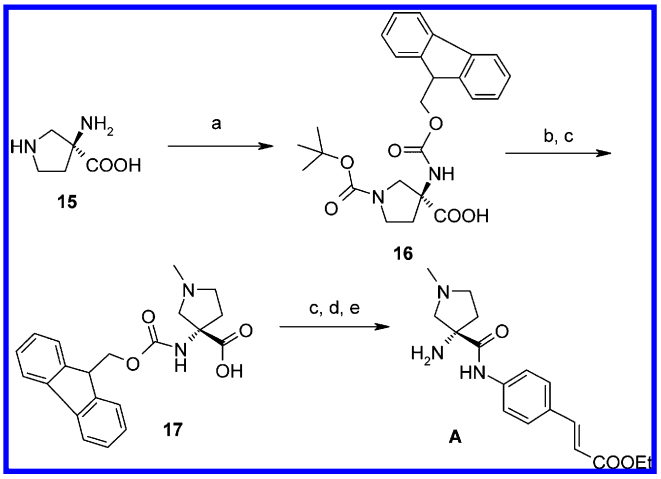

[a](a) Di-*tert*-butyl dicarbonate, NaOH, THF, rt, then Fmoc-OSu; (b) TFA, CH_2Cl_2, rt; (c) 37% aqueous formaldehyde, $NaBH_3CN$, EtOH, AcOH; (d) ethyl 4-aminocinnamate, HATU, HOAt, 2,4,6-collidine, DMF, 50 °C; (e) DBU, THF, rt.

tert-butoxycarbonyl derivative (Boc) on the pyrrolidine ring nitrogen and an Fmoc carbamate on the remaining amino function (compound **16**). Carboxylic acid **16** was then coupled to ethyl 4-aminocinnamate to give amide **17**. Following cleavage of the Boc protecting group, the pyrrolidine nitrogen was methylated and the Fmoc protecting group removed under standard conditions to provide the right-hand-side fragment **A**, protected as the ethyl ester (Scheme 5). Right-hand side **B** was prepared in a similar fashion starting from commercially available Boc/Fmoc differentially protected 4-aminopiperidine-4-carboxylic acid.

Ethyl 4-aminocinnamate ester building blocks **C**, **D**, and **E** were obtained by condensation of ethyl 4-aminocinnamate with amino acid chlorides **18**, themselves obtained from commercially available amino acids using the procedure of Rorrer et al., as shown in Scheme 6.[33] Fragment **H** was prepared in a similar fashion starting from *α*-methylcinnamic acid **19** via sequential protection of the acid function and reduction of the nitro group to give aniline **20**. Coupling with **18** (n = 1) gave the desired right-hand-side building block **H**.

Inhibitors were prepared from indole-6-carboxylic acids (Chart 1) and amine fragments **A**–**H** (Chart 2) using standard peptide coupling procedures and purified by reversed-phase HPLC following saponification of the carboxylic ester under basic conditions as described in Scheme 7. Inhibitor characterization data are provided in the Supporting Information.

Scheme 7. Final Assembly of Inhibitors[a]

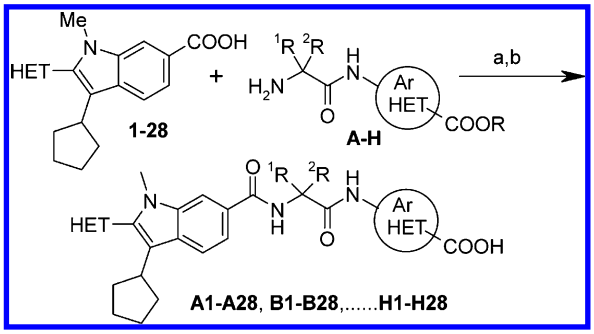

[a](a) TBTU or HATU, Et_3N or DIEA, DMSO, rt; (b) LiOH or NaOH, water–DMSO or water–THF–MeOH, rt.

CONCLUSION

The overall ADME-PK profile of indole-based HCV NS5B thumb pocket 1 inhibitors was improved by replacing the 3-cyclohexyl moiety of these inhibitors by a metabolically more stable cyclopentyl group. By use of parallel synthesis techniques, a sparse matrix of more than 100 inhibitors was generated from combinations of C2 indole substituents and amide right-hand sides, approximately 50 of which had gt1b replicon EC_{50} < 100 nM. Microsome metabolic stability and Caco-2 permeability filters were then applied to select 71 analogues for oral screening in rat cassettes. Of these, compound **D13** provided the most optimal balance between antiviral potency (the complete preclinical profile of **D13** will be reported elsewhere) and a consistent cross-species PK profile and was selected for development followed by a clinical proof-of-concept study in HCV-infected patients.

Scheme 6. Synthesis of C–E Right-Hand Sides[a]

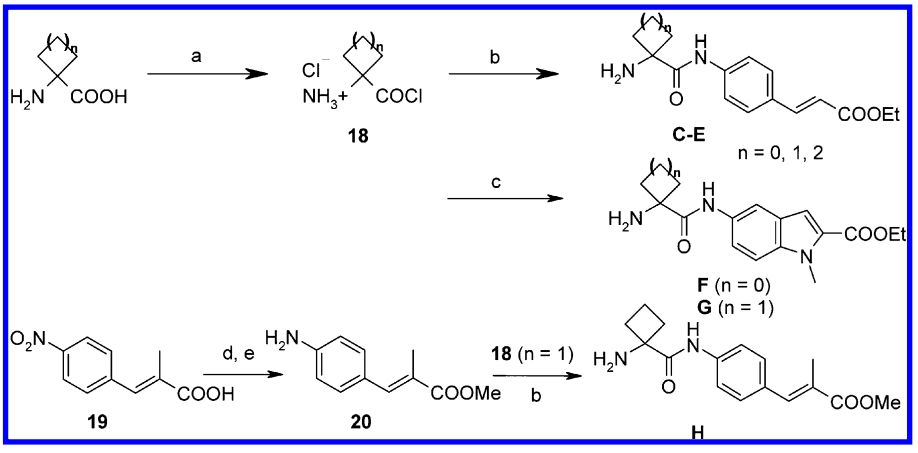

[a](a) 2-Oxazolidone, PCl_5, MeCN, rt; (b) ethyl 4-aminocinnamate, K_3PO_4, MeCN, rt; (c) ethyl 5-amino-1-methyl-1*H*-indole-2-carboxylate, pyridine, CH_2Cl_2, rt; (d) CH_2N_2, diethyl ether–MeOH, 0 °C; (e) $SnCl_2$ dihydrate, EtOH, reflux.

dx.doi.org/10.1021/jm3006788 | *J. Med. Chem.* 2012, 55, 7650–7666

EXPERIMENTAL SECTION

General Experimental. All commercially obtained solvents and reagents were used as received without further purification. All reactions were carried out under an atmosphere of argon. Temperatures are given in °C. Solution percentages express a weight to volume relationship, and solution ratios express a volume to volume relationship, unless stated otherwise. NMR spectra were recorded on a Bruker AVANCE II (400 MHz for ^{1}H NMR) spectrometer and were referenced to either DMSO-d_6 (2.50 ppm) or $CDCl_3$ (7.27 ppm). Data are reported as follows: chemical shift (ppm), multiplicity (s = singlet, d = doublet, t = triplet, br = broad, m = multiplet), coupling constant (J, reported to the nearest 0.5 Hz), and integration. Mass spectra were obtained from a Micomass AutoSpec instrument using ES as ionization mode. Purification of crude material was performed either by flash column chromatography or by using a CombiFlash Companion using RediSep silica or SilicaSep columns according to preprogrammed gradient and flow rate separation conditions in hexane/EtOAc or DCM/MeOH. The final compounds were purified by preparative HPLC on a Waters 2767 sample manager with pumps 2525, column fluidics organizer (CFO), PDA detector 2996, and MassLynx 4.1 using either a Whatman Partisil 10-ODS-3 column, 2.2 cm × 50 cm or a YMC Combi-Prep ODS-AQ column, 50 mm × 20 mm i.d., S, 5 μm, 120 Å, and a linear gradient program from 2% to 100% AcCN/water (0.06% TFA). Fractions were analyzed by analytical HPLC, and the pure fractions were combined, concentrated, frozen, and lyophilized to yield the desired compound as a neutral entity or the trifluoroacetate salt for basic analogues. Inhibitor HPLC purity was measured by using a Waters Alliance 2695 separation module with a Waters TUV 2487 UV detector. The column was a Combiscreen ODS-AQ, 5 μm, 4.6 mm × 50 mm, linear gradient from 5% to 100% ACN/H_2O + 0.06% TFA in 10.5 min, detection at 220 nm. All final inhibitors had HPLC homogeneity of ≥95% unless noted otherwise (see Supporting Information).

3-(1-Cyclopentenyl)indole-6-carboxylic Acid 8. A 3 L three-neck flask equipped with a reflux condenser and mechanical stirrer was charged with indole-6-carboxylic acid **7** (purchased from Peakdale Intermediates, 220.0 g, 1.365 mol) and KOH pellets (764.45 g, 13.65 mol, 10 equiv). Water (660 mL) and MeOH (660 mL) were added, and the stirred mixture was heated to 75 °C. Cyclopentanone (603.7 mL, 6.825 mol, 5 equiv) was added dropwise over 18 h. The mixture was then stirred for an additional 3 h and cooled to 0 °C. The precipitated potassium salt was collected by filtration and washed with *tert*-butyl methyl ether (TBME, 2 × 500 mL) to remove cyclopentanone self-condensation byproduct. The brown solid was redissolved in water (2.5 L) and the solution washed with additional TBME (2 × 1 L). Following acidification of the aqueous phase to pH 3 with concentrated HCl (425 mL), the beige precipitate was collected by filtration, washed with water (2 × 1 L), and dried to constant weight under vacuum at 70 °C (279.5 g, 88.9% yield). The crude was used as such in the next step: ^{1}H NMR (400 MHz, DMSO-d_6) δ 12.52 (broad s, 1H), 11.50 (s, 1H), 8.02 (d, J = 0.8 Hz, 1H), 7.88 (d, J = 8.6 Hz, 1H), 7.66 (dd, J = 8.4, 1.4 Hz, 1H), 7.57 (d, J = 2.6 Hz, 1H), 6.16 (s, 1H), 2.71 (m, 2H), 2.53 (m, 2H), 1.92 (m, 2H). ^{13}C NMR (100 MHz, DMSO-d_6) δ 168.2, 136.2, 128.3, 127.5, 123.5, 121.1, 120.3, 119.7, 113.7, 113.0, 38.2, 34.4, 33.2, 22.2. ES-MS(−) m/z 225.9 (M − H).

3-Cyclopentylindole-6-carboxylic Acid 9. Crude cyclopentenylindole **8** from above (159.56 g, 0.70 mol) was dissolved in MeOH (750 mL), and the solution was purged with argon gas. 20% $Pd(OH)_2$ on charcoal (Pearlman's catalyst, 8.0 g) was added, and the suspension was hydrogenated in a Parr apparatus under 50 psi of hydrogen gas for 18 h. After completion, the suspension was again purged with argon, and the catalyst was removed by filtration through a pad of Celite and the solvent removed under reduce pressure. The resulting brown solid was dried at 70 °C under vacuum to constant weight, providing crude cyclopentylindole analogue **9** as a beige solid (153.2 g): ^{1}H NMR (400 MHz, DMSO-d_6) δ 12.40 (broad s, 1H), 11.12 (s, 1H), 7.98 (s, 1H), 7.60 (d, J = 8.3 Hz, 1H), 7.57 (dd, J = 8.3, 1.2 Hz, 1H), 7.34 (d, J = 1.5 Hz, 1H), 3.22 (quintet, J = 7.6 Hz, 1H), 2.09 (m, 2H), 1.77 (m, 2H), 1.64 (m, 4H). ^{13}C NMR (100 MHz, DMSO-d_6) δ 168.4, 135.8, 130.0, 124.5, 122.9, 119.5, 119.0, 118.4, 113.5, 36.4, 32.9, 24.8. ES-MS(−) m/z 228.0 (M − H).

3-Cyclopentyl-1-methylindole-6-carboxylic Acid Methyl Ester 10. A 3 L three-neck flask equipped with a mechanical stirrer and thermometer was charged with crude 3-cyclopentyl-6-indolecarboxylic acid **9** (74.00 g, 0.323 mol) and purged with nitrogen. Anhydrous DMF (740 mL) was added and the mixture stirred until dissolution of solids. Anhydrous K_2CO_3 (66.91 g, 0.484 mol, 1.5 equiv) was added followed by MeI (50 mL, 0.807 mol, 2.5 equiv). After the mixture was stirred at room temperature for 5 h, HPLC analysis indicated complete conversion to the methyl ester. The reaction mixture was cooled in an ice bath, and NaH (95%, oil-free, 10.10 g, 0.42 mol, 1.3 equiv) was added in small portions. After the mixture was stirred for an additional 15 min, the ice bath was removed and the mixture was stirred for an additional 1.5 h at room temperature (no more progress by HPLC). Additional NaH (1.55 g, 65 mmol, 0.2 equiv) and MeI (1.0 mL, 16 mmol, 0.05 equiv) were added, and after the mixture was stirred for an additional 15 min, the reaction was judged to be complete. The reaction mixture was poured into water (4 L) and acidified to pH < 2 with concentrated HCl (85 mL). The solution was adjusted to pH 7 with 4 N NaOH (40 mL), and after the mixture was stirred overnight at room temperature, the precipitated solid was collected by filtration, washed with water (600 mL), and dried to constant weight under vacuum. The crude product (72.9 g) contains a poorly soluble impurity resulting from carried-over dimerization of the indole (impurity **11**) that was removed by successive triturations with organic solvents as follows: the crude material was triturated with hot MeOH (~250 mL). After cooling in ice, the solid was collected and redissolved in a minimum amount of hot EtOAc (~300 mL). After the solution was cooled to room temperature, hexane (1.5 L) was added and the mixture stirred overnight at room temperature. Undissolved solids were removed by filtration and the filtrate was evaporated under reduced pressure to give the desired *N*-methylindole ester **10** as a beige solid (47 g, 57% yield): mp 113−114.5 °C. ^{1}H NMR (400 MHz, DMSO-d_6) δ 8.02 (s, 1H), 7.64 (d, J = 8.4 Hz, 1H), 7.62 (dd, J = 8.4, 1.0 Hz, 1H), 7.36 (s, 1H), 3.86 (s, 3H), 3.80 (s, 3H), 3.20 (quintet, J = 8.0 Hz, 1H), 2.10 (m, 2H), 1.77 (m, 2H), 1.72−1.55 (m, 4H). ^{13}C NMR (100 MHz, DMSO-d_6) δ 167.3, 136.1, 130.6, 129.4, 121.9, 118.9, 118.8, 111.6, 51.8, 36.2, 33.0, 32.4, 24.7. ES-MS(−) m/z 227.9 (M − H). Anal. Calcd for $C_{16}H_{19}NO_2$: C, 74.68; H, 7.44; N, 5.44. Found: C, 74.40; H, 7.36; N, 5.42.

2-Bromo-3-cyclopentyl-1-methylindole-6-carboxylic Acid Methyl Ester 12. *N*-Methylindole ester **10** (80.70 g, 0.31 mol) was dissolved in isopropyl acetate (1.2 L), and the mechanically stirred solution was treated with NaOAc (38.59 g, 0.47 mol, 1.5 equiv) and cooled to 4 °C. Bromine (16.87 mL, 0.33 mol, 1.1 equiv) was added dropwise over 6 min, and the resulting suspension was stirred for an additional 50 min at 13 °C. Additional bromine (3.2 mL, 63 mmol, 0.2 equiv) was then added, and after the mixture was stirred for 20 min, the reaction was determined to be complete (HPLC). The reaction was then quenched by addition of 10% aqueous sodium thiosulfate (125 mL), followed by water (400 mL) and K_2CO_3 (78 g, 1.8 equiv). The biphasic mixture was stirred for 10 min, and the organic phase was separated. It was washed with 10% sodium thiosulfate solution (80 mL) and 1 M K_2CO_3 (80 mL) and dried ($MgSO_4$). The dried extract was evaporated under reduced pressure to yield a beige solid (109.5 g). The crude material was suspended in MeOH (750 mL) and the mixture refluxed for 30 min. After the mixture was cooled in an ice bath, the beige solid was collected by filtration, washed with cold MeOH (200 mL), and dried to constant weight under vacuum at 60 °C (73.4 g, 79% yield): mp 110−111 °C. ^{1}H NMR (400 MHz, DMSO-d_6) δ 8.09 (s, 1H), 7.67 (d, J = 8.4 Hz, 1H), 7.64 (dd, J = 8.4, 1.2 Hz, 1H), 3.87 (s, 3H), 3.80 (s, 3H), 3.26 (quintet, J = 9.8 Hz, 1H), 1.90 (m, 6H), 1.70 (m, 2H). ^{13}C NMR (100 MHz, DMSO-d_6) δ 167.0, 136.1, 128.5, 122.3, 118.7, 118.4, 117.2, 116.8, 111.9, 51.9, 37.5, 31.9, 31.7, 25.7. ES-MS(+) m/z 336.0 and 338.0 (MH^+). Anal. Calcd for $C_{16}H_{18}BrNO_2$: C, 57.16; H, 5.40; N, 4.17. Found: C, 57.29; H, 5.25; N, 3.96.

dx.doi.org/10.1021/jm3006788 | J. Med. Chem. 2012, 55, 7650−7666

Methyl Ester of 3-Cyclopentyl-2-(3-furyl)-*N*-methylindole-6-carboxylic Acid (Methyl Ester of Building Block 1) via Suzuki–Miyaura Cross-Coupling (Method A). 2-Bromoindole **12** (2.03 g, 6.0 mmol) was combined with 3-furylboronic acid (1.014 g, 9.1 mmol), sodium carbonate (1.28 g, 12 mmol), and LiCl (0.51 g, 12 mmol) in a round-bottomed flask equipped with a reflux condenser. Toluene (20 mL), ethanol (20 mL), and water (16 mL) were added, and the dark heterogeneous mixture was degassed by bubbling a stream of argon through the mixture for 15 min. $Pd(PPh_3)_4$ (350 mg, 0.3 mmol) was added and the mixture heated to 80 °C under an argon atmosphere. After 3 h (60% conversion by HPLC analysis), another portion of $Pd(PPh_3)_4$ (350 mg, 0.3 mmol) was added and heating continued overnight (>90% conversion). The reaction mixture was cooled to room temperature, diluted with EtOAc and the solution washed with saturated aqueous NH_4Cl and brine. The organic phase was dried ($MgSO_4$) and concentrated under reduced pressure to give a residue that was purified by flash chromatography using 1:19 EtOAc/hexane as eluent. The methyl ester of building block **1** was recovered as a white foam (1.66 g, 57% yield): mp 79–82 °C. R_f = 0.24 (1:19 EtOAc/hexane). ^{1}H NMR (400 MHz, DMSO-d_6) δ 8.09 (d, J = 0.9 Hz, 1H), 7.98 (s, 1H), 7.91 (t, J = 1.7 Hz, 1H), 7.69 (d, J = 8.4 Hz, 1H), 7.64 (dd, J = 8.4, 1.3 Hz, 1H), 6.76 (d, J = 1.1 Hz, 1H), 3.87 (s, 3H), 3.67 (s, 3H), 3.13 (m, J = 8.9 Hz, 1H), 1.78 (m, 6H), 1.64 (m, 2H). ^{13}C NMR (100 MHz, DMSO-d_6) δ 167.2, 144.0, 142.7, 136.5, 132.6, 128.8, 121.9, 119.2, 119.1, 116.8, 115.4, 112.2, 111.8, 51.8, 36.9, 32.8, 30.6, 25.8. ES-MS(+) m/z 324.1 (MH^+).

3-Cyclopentyl-1-methyl-2-tributylstannanyl-1*H*-indole-6-carboxylic Acid Methyl Ester 13. A 3 L three-necked flask fitted with a mechanical stirrer, low temperature thermometer, and addition funnel was purged with argon gas. 2-Bromoindole 12 (82.73 g, 246 mmol, 1 equiv) was added followed by anhydrous THF (1 L). The solution was cooled to −72 °C. *n*-BuLi in hexane (2.5 M, 100 mL, 250 mmol, 1.016 equiv) was added dropwise keeping the internal temperature below −68 °C (35–40 min). After the mixture was stirred for 5 min, HPLC analysis of an aliquot quenched in MeOH showed no more starting material. Bu_3SnCl (83.41 mL, 308 mmol, 1.25 equiv) was added neat dropwise over 30 min, keeping the internal temperature below −68 °C. The mixture was stirred at −72 °C for 30 min and then allowed to warm to room temperature. Volatiles were removed under reduced pressure, and the residue was dissolved in TBME (1.5 L). The organic phase was washed with a mixture of 5% citric acid (150 mL) and brine (150 mL) and then with 5% $NaHCO_3$ (150 mL) and brine (150 mL). After a final washing with brine (150 mL), the organic phase was dried (Na_2SO_4) and concentrated to a black viscous oil.

Silica gel (1.2 kg, 230–400 mesh) was slurried with 5% triethylamine in hexane (6 L) and charged into a 12 cm diameter column. The solvent was passed several times through the silica to ensure complete deactivation and then discarded (3.3 L). The crude stannane from above was dissolved in fresh 5% Et_3N/hexane (200 mL) and charged onto the column. The material was eluted with the same solvent (6 L), and fractions containing the product were pooled. Evaporation of volatiles under reduced pressure gave stannane **13** as a yellow oil (104.9 g): ^{1}H NMR (400 MHz, DMSO-d_6) δ 8.07 (s, 1H), 7.73 (d, J = 8.4 Hz, 1H), 7.66 (d, J = 8.4 Hz, 1H), 3.97 (s, 3H), 3.83 (s, 3H), 3.11 (quintet, J = 9.0 Hz, 1H), 2.09 (m, 2H), 1.97 (m, 4H), 1.78 (m, 2H), 1.58 (m, 6H), 1.38 (m, J = 7.2 Hz, 6H), 1.21 (m, 6H), 0.93 (t, J = 7.2 Hz, 9H). ^{13}C NMR (100 MHz, DMSO-d_6) δ 168.5, 144.6, 140.4, 129.4, 128.9, 122.2, 119.1, 118.8, 111.5, 51.8, 40.7, 34.0, 33.9, 29.0, 27.3, 26.6, 13.6, 11.5. ES-MS(+) m/z 548.3 (MH^+).

Methyl Ester of 3-Cyclopentyl-2-(2-pyridyl)-*N*-methylindole-6-carboxylic Acid (Methyl Ester of Building Block 13) via Stille Cross-Coupling (Method B). Stannane 13 (104.60 g, 191.5 mmol) was dissolved in dry DMF (500 mL). Triphenylphosphine (50.31 g, 191.8 mmol, 1.0 equiv), CuI (3.653 g, 19.18 mmol, 0.1 equiv), LiCl (16.26 g, 383.6 mmol, 2 equiv), and 2-bromopyridine (23.77 mL, 249.4 mmol, 1.3 equiv) were added. The suspension was purged by bubbling argon through for 45 min. Tetrakistriphenylphosphine Pd^0 (5.00 g, 4.327 mmol, 2.3 mol %) was added and the mixture heated to 100 °C. After the mixture was stirred at that temperature for 2 h, Et_3N-deactivated TLC analysis indicated complete reaction. The mixture was cooled, and the DMF phase was washed with hexane (3 × 250 mL). DMF (350 mL) was removed under vacuum, and water (1 L) was added followed by TBME (500 mL). A precipitate of triphenylphosphine formed in the biphasic system. It was removed by filtration and washed with TBME. The filtrate and washings from above were combined, and the organic phase was separated. The aqueous phase was extracted again with TBME (2 × 500 mL), and the extracts were combined. After the mixture was washed with brine (300 mL) and dried ($MgSO_4$), volatiles were removed to give a dark red syrup.

To the above material was added TBME (100 mL) and hexane (300 mL) and the solution chilled to 0 °C to induce crystallization. The mixture was then further cooled to −20 °C and the solid collected by filtration. It was washed with hexane and dried to give the desired product (28.20 g) as a brown-reddish solid (94–95% homogeneity by HPLC). The filtrate and washings from above were combined, and the remaining product was isolated by chromatography on silica gel (1 kg, 230–400 mesh) using $CHCl_3$ and then 10–20% EtOAC–$CHCl_3$ as eluents. Additional product (23.55 g) of comparable homogeneity to the first crop was obtained as a yellow solid (total yield of 51.75 g, 80%): mp 114–115 °C. ^{1}H NMR (400 MHz, DMSO-d_6) δ 8.80 (d, J = 4.5 Hz, 1H), 8.14 s, 1H), 7.99 (dd, J = 1.6, 7.6 Hz, 1H), 7.77 (d, J = 8.4 Hz, 1H), 7.68 (d, J = 8.4 Hz, 1H), 7.59 (d, J = 7.6 Hz, 1H), 7.49 (dd, J = 7.6, 4.9 Hz, 1H), 3.89 (s, 3H), 3.69 (s, 3H), 3.14 (m, 1H), 1.88 (m, 6H), 1.62 (m, 2H). ^{13}C NMR (100 MHz, DMSO-d_6) δ 167.1, 150.2, 149.7, 139.3, 136.8, 136.6, 128.6, 126.2, 123.1, 122.6, 119.8, 119.3, 117.2, 112.1, 51.8, 36.7, 32.8, 30.9, 25.8. ES-MS(+) m/z 335.2 (MH^+).

Methyl Ester of 3-Cyclopentyl-2-(2-pyridyl)-*N*-methylindole-6-carboxylic Acid, Hydrochloride (Methyl Ester of Building Block 13) via in Situ Generation of 2-Indole Boronate and Suzuki–Miyura Cross-Coupling (Method C). *n*-Butyllithium (1.6 M in hexane, 97.4 mL, 1.05 equiv) was added to a solution of bromoindole **12** (50.0 g, 148.7 mmol, 1.00 equiv) in THF (250 mL), maintaining the temperature of the mixture below −71 °C. After the mixture was stirred at this temperature for 10 min, HPLC analysis showed that the starting bromoindole had completely reacted. Trimethyl borate (20.2 mL, 1.2 equiv) was added, maintaining the temperature below −69 °C. After being stirred at this temperature for 0.5 h, the mixture was warmed to 0 °C and stirred for an additional 1 h, when it was allowed to warm to room temperature. HPLC analysis showed the formation of a mixture of the desired boronate and the 2-H indole side product in the ratio 93.9:5.3. To the reaction mixture was added 250 mL of THF (250 mL), tri-*p*-tolylphosphine (2,72 g, 0.06 equiv), and 2-bromopyridine (28.1 g, 1.2 equiv). The resulting solution was purged with argon for 30 min. Palladium acetate (333.0 mg, 0.01 equiv) was added and the solution stirred for 10 min. Then potassium carbonate (40.9 g, 2 equiv) was added followed by methanol (165 mL). The reaction mixture was then heated at reflux under an argon atmosphere for 4.5 h. HPLC analysis showed that about 1% of the starting boronate was left after 3 and 4.5 h of reaction. The reaction mixture was allowed to cool to room temperature and the solvent removed under reduced pressure. The residue was taken up in MTBE (250 mL) to which was then added water (250 mL), and the biphasic mixture was stirred for 10 min. The layers were then separated, and the organic layer was washed with brine (50 mL), dried over anhydrous magnesium sulfate, and filtered through a glass frit. The filtrate was carefully treated with 4.0 M HCl and 1,4-dioxane solution (50 mL, 1.3 equiv). The solvent was removed under reduced pressure, and MTBE (500 mL) and dichloromethane (450 mL) were added. The mixture was warmed to reflux temperature. Then additional dichloromethane (900 mL) was added and the temperature again raised to reflux in order to achieve complete solution. The mixture was cooled to 10 °C and the solid collected by filtration. The solid product was dried in a vacuum oven at 40 °C to afford 35.6 g of product. The filtrate was evaporated and then treated with a 1:1 mixture of MTBE/DCM (600 mL total volume), cooled to 10 °C and the solid collected by filtration. This material was dried in a vacuum oven to afford a further 11.0 g of product. The combined solids (46.56

dx.doi.org/10.1021/jm3006788 | J. Med. Chem. 2012, 55, 7650–7666

g, 84% yield, 94% purity by HPLC) were identical in all respects to material generated using the Stille procedure.

3-Cyclopentyl-1-methyl-2-pyridin-2-yl-1*H*-indole-6-carboxylic Acid (Building Block 13). The two product crops of the methyl ester of building block **13** from Stille cross-coupling of bromoindole **12** with 2-bromopyridine (51.0 g, 154.7 mmol) were dissolved in a mixture of THF (100 mL) and MeOH (100 mL), and the solution was heated to 60 °C. Then 5 N NaOH (125 mL) was added portionwise over 15 min and the mixture stirred for 1 h at 60 °C after which HPLC analysis showed complete hydrolysis. The reaction mixture was cooled to room temperature, and organics were removed under reduced pressure to give a pink suspension. Water (1 L) was added and the mixture stirred for 30 min before the solid was removed by filtration. The filtrate was washed with TBME (3 × 250 mL) and hexane (250 mL), and concentrated HCl (40 mL) was added slowly with stirring to the aqueous phase. AcOH (15 mL) was then added slowly to form a white precipitate. After the mixture was stirred for 30 min, the precipitated product was collected by filtration, washed with water, and dried under vacuum at 60 °C (43.2 g, 87% yield): mp 237−238.5 °C. ^{1}H NMR (400 MHz, DMSO-d_6) δ 12.61 (broad s, 1H), 8.80 (d, J = 4.3 Hz, 1H), 8.12 (s, 1H), 7.98 (dt, J = 7.6, 1.6 Hz, 1H), 7.74 (d, J = 8.4 Hz, 1H), 7.67 (d, J = 8.2 Hz, 1H), 7.58 (d, J = 7.8 Hz, 1H), 7.48 (dd, J = 7.4, 5.1 Hz, 1H), 3.68 (s, 3H), 3.15 (quintet, J = 9.3 Hz, 1H), 1.89 (m, 6H), 1.62 (m, 2H). ^{13}C NMR (100 MHz, DMSO-d_6) δ 168.2, 150.3, 149.7, 139.0, 136.8, 136.7, 128.3, 126.2, 123.8, 123.1, 119.64, 119.61, 117.1, 112.2, 36.7, 32.8, 30.8, 25.8. ES-MS(+) m/z 321.2 (MH^+).

1-Chlorocarbonylcyclobutylammonium Chloride 18 (n = 1). A 3 L three-necked flask equipped with a mechanical stirrer was purged with nitrogen and charged with 2-oxazolidone (81.7 g, 938 mmol, 1.22 equiv) and acetonitrile (1.2 L). Phosphorus pentachloride (260 g, 1.25 mol, 1.63 equiv) was added in one portion (no exotherm noticed), and the mixture was stirred 14 h at room temperature. 1-Aminocyclobutanecarboxylic acid (88.5 g, 769 mmol, 1 equiv) was added and the resulting suspension stirred for 22 h. The suspended solid was collected by suction filtration, washed with acetonitrile (200 mL), and dried under vacuum (105.1 g, 80% yield). Anal. Calcd for $C_5H_9Cl_2NO$: C, 35.32; H, 5.33; N, 8.24. Found: C, 35.54; H, 5.48; N, 8.30. Material partially decomposed upon standing for extended periods of time (>1 month). This procedure was adapted to the preparation of other amino acid chloride hydrochlorides (e.g., derived from 1-aminocyclopentanecarboxylic acid).

(*E*)-3-{4-[(1-Aminocyclobutanecarbonyl)amino]phenyl}-acrylic Acid Ethyl Ester (Ethyl Ester of Building Block D). Acid chloride **18** (41.1 g, 242 mmol, 1.20 equiv) was suspended in acetonitrile (400 mL), and ethyl 4-aminocinnamate (38.52 g, 201 mmol, 1.0 equiv) was added. After the mixture was stirred for 30 min, HPLC showed 95% conversion. Additional acid chloride (2.70 g, 16 mmol, 0.08 equiv) was added, and after the mixture was stirred for an additional 20 min, conversion was judged to be complete. After the mixture was stirred for an additional 90 min (2.5 h total reaction time), solid K_3PO_4 (106.9 g, 504 mmol, 2.5 equiv) was added, and after the mixture was stirred for 15 min, the reaction mixture was poured into water (2 L). After the mixture was stirred for 20 min (pH ~8), the precipitated product was collected by filtration, rinsed with water (250 mL), and dried in vacuum at 60 °C (55.9 g, 96% yield): mp 122−124.5 °C. ^{1}H NMR (400 MHz, DMSO-d_6) δ 7.75 (d, J = 8.8 Hz, 2H), 7.66 (d, J = 8.8 Hz, 2H), 7.58 (d, J = 15.9 Hz, 1H), 6.52 (d, J = 16.1 Hz, 1H), 4.18 (q, J = 7.1 Jz, 2H), 2.5 (m, 2H), 1.9 (m, 3H), 1.75 (m, 1H), 1.25 (t, J = 7.1 Hz, 3H). ^{13}C NMR (100 MHz, DMSO-d_6) δ 175.2, 166.4, 144.0, 141.0, 129.1, 128.7, 119.1, 116.1, 59.8, 59.4, 33.6, 14.2, 13.8. ES-MS(+) m/z 289.1 (MH^+).

D13 Ethyl Ester. Indole building block **13** (43.00 g, 134.2 mmol, 1 equiv) and amine fragment **D** (40.63 g, 140.9 mmol, 1.05 equiv) were dissolved in DMSO (200 mL), and triethylamine (74.8 mL, 537 mmol, 4 equiv) was added followed by TBTU (64.62 g, 201 mmol, 1.5 equiv). A slight exotherm was noticed. The mixture was stirred for 16 h at room temperature (seemed complete after 2 h as shown by HPLC). The reaction mixture was then added dropwise in a vigorously stirred mixture of water (2 L), NaCl (300 g), and AcOH (40 mL). The precipitated cream-colored solid was centrifuged and the aqueous phase carefully decanted out. The solids were resuspended in a mixture of water (2 L) and NaCl (300 g). The solid material was separated from the water as before, dissolved in EtOAc (1 L), and washed with 1 N NaOH (2 × 250 mL), saturated aqueous $NaHCO_3$ (250 mL), and brine (250 mL). The extract was dried ($MgSO_4$) and evaporated to a yellow paste (the product begins to crystallize during the concentration process). TBME (300 mL) and $CHCl_3$ (50 mL) were added, and the slurry was heated to 60 °C for 30 min. Hexane (1000 mL) was added portionwise to the hot slurry, and heating continued for an additional 30 min. The mixture was allowed to cool to room temperature and then to 10 °C. The solid ester product (**D13** ethyl ester) was collected by filtration, washed with 20% TBME in hexane, and dried in vacuum at 60 °C (70.0 g, 88% yield): ^{1}H NMR (400 MHz, DMSO-d_6) δ 9.74 (s, 1H), 8.86 (s, 1H), 8.81 (d, J = 3.9 Hz, 1H), 8.22 (s, 1H), 7.99 (dt, J = 7.6, 1.6 Hz, 1H), 7.74−7.54 (m, 8H), 7.49 (dd, J = 7.4, 4.9 Hz, 1H), 6.50 (d, J = 16 Hz, 1H), 4.16 (q, J = 7.0 Hz, 2H), 3.73 (s, 3H), 3.16 (m, 1H), 2.74 (m, 2H), 2.38 (m, 2H), 2.05−1.80 (m, 8H), 1.63 (m, 2H), 1.24 (t, J = 7.0 Hz, 3H). ^{13}C NMR (100 MHz, DMSO-d_6) δ 172.2, 166.9, 166.3, 150.5, 149.7, 144.0, 141.4, 138.3, 136.8, 129.0, 128.6, 127.3, 127.0, 126.2, 122.9, 119.4, 119.3, 118.4, 117.0, 116.1, 110.4, 59.84, 59.79, 36.7, 32.9, 31.0, 30.7, 25.8, 15.0, 14.2. ES-MS(+) m/z 591.4 (MH^+).

(*E*)-3-[4-({1-[(3-Cyclopentyl-1-methyl-2-pyridin-2-yl-1*H*-indole-6-carbonyl)amino]cyclobutanecarbonyl}amino)phenyl]-acrylic Acid (D13). **D13** ethyl ester (66.00 g) was dissolved in DMSO (200 mL) and the solution heated to 60 °C. Then 5 N NaOH (66 mL, 3 equiv) was added dropwise over 10 min and the mixture heated for an additional 15 min at 60 °C (hydrolysis complete by HPLC). The reaction mixture was cooled to room temperature and added dropwise to a well stirred mixture of water (2 L), NaCl (300 g), and AcOH (25 mL). A precipitate formed in a dark reddish-brown solution. The solid was collected by filtration and washed with water (600 mL). The solid pastelike material was dissolved in EtOAc (1.2 L) and the organic portion washed with brine (2 × 500 mL). After the mixture was dried (Na_2SO_4), removal of the solvent under reduced pressure gave a solid that was suspended in absolute EtOH (200 mL). The mixture was warmed with stirring to 65−70 °C. While hot, $CHCl_3$ (300 mL) was added in portions. The mixture was refluxed until all solids dissolved. The solution was stirred at 65−70 °C, allowing the product to slowly crystallize out. After 1 h, TBME (1 L) was added dropwise (1 h), maintaining a gentle reflux throughout. The thick suspension was stirred for an additional 1 h at reflux and then slowly cooled to room temperature. The solid was collected by filtration, washed with 20% $CHCl_3$ in TBME (200 mL) and then TBME (2 × 200 mL), and dried under vacuum at 60 °C (53.69 g).

The crude material from above was suspended in absolute EtOH (200 mL) and then warmed to 70 °C. To the suspension was added TBME (1.3 L) in 100 mL portions over 10 min. The mixture was refluxed for 1 h and cooled to room temperature. The cream-colored solid was collected by filtration, washed with TBME (3 × 200 mL), and dried in vacuum at 60 °C for 84 h (50.40 g, 80% yield): mp 252−256 °C. ^{1}H NMR (400 MHz, DMSO-d_6) δ 12.22 (broad s, 1H), 9.70 (s, 1H), 8.84 (s, 1H), 8.80 (d, J = 4.7 Hz, 1H), 7.73−7.46 (m, 9H), 6.39 (d, J = 16.0 Hz, 1H), 3.73 (s, 3H), 3.16 (quintet, J = 8.8 Hz, 1H), 2.74 (m, 2H), 2.37 (m, 2H), 1.98 (m, 1H), 1.89 (m, 6H), 1.62 (m, 2H). ^{13}C NMR (100 MHz, DMSO-d_6) δ 172.2, 167.7, 167.0, 150.5, 149.7, 143.6, 141.3, 138.3, 136.8, 136.7, 128.8, 127.4, 127.1, 126.2, 122.9, 119.5, 119.4, 118.5, 117.2, 117.1, 110.4, 59.9, 36.8, 32.9, 31.0, 30.8, 25.9, 15.1. ES-MS(+) m/z 563.4 (MH^+).

2-(2-Bromoacetyl)-3-cyclopentyl-1-methyl-1*H*-indole-6-carboxylic Acid Methyl Ester 14. To bromoindole **12** (7.66 g, 23.0 mmol) in dioxane (130 mL) in a 250 mL round-bottomed flask was added 1-ethoxyvinlytributlytin (10.0 g, 28.0 mmol). The mixture was degassed by bubbling argon gas through the homogeneous mixture for a period of 30 min. Di(triphenylphosphine)palladium dichloride (1.3 g, 1.9 mmol) was added and the mixture degassed for a further 10 min. The mixture was then heated to reflux and stirred for 20+ h. The reaction was judged to be complete by TLC, and the mixture was cooled to room temperature. The volatiles were removed under

reduced pressure, and the residue was absorbed onto silica gel. The intermediate ethoxyvinylindole was purified by flash chromatography on silica using 4% EtOAc/hexane as eluent to afford 6.49 g of the ethoxyvinylindole derivative that was used directly in the next step.

The ethoxyvinylindole from above was dissolved in THF (65 mL). To this was added water (6.5 mL), and the mixture was cooled in an ice/water bath. *N*-Bromosuccinimide (3.53 g, 19.8 mmol) was added in small portions over a period of 50 min, and stirring continued for a further 30 min, after which the reaction was judged to be complete by TLC. The mixture was diluted with diethyl ether (200 mL), and water was added (200 mL). The phases were separated, and the aqueous layer was washed with 2 × 80 mL of diethyl ether. The organic portions were combined, washed with brine, dried over Na_2SO_4, filtered, and evaporated. The residue was purified on silica gel, using a 5−15% EtOAc/hexane gradient to provide 5.30 g of bromomethyl ketone **14** (61% yield for both steps): mp 115−118 °C (dec). ^{1}H NMR (400 MHz, $CDCl_3$) δ 8.13 (broad t, J = 0.4 Hz, 1H), 7.79 (dd, J = 8.6, 0.9 Hz, 1H), 7.76 (dd, J = 8.6, 1.3 Hz, 1H), 4.43 (s, 2H), 3.97 (s, 3H), 3.86 (s, 3H), 3.47 (m, J = 8.6 Hz, 1H), 2.15−2.0 (m, 6H), 1.85 (m, 2H). ^{13}C NMR (100 MHz, $CDCL_3$) δ 188.5, 167.5, 139.1, 134.4, 127.8, 126.7, 126.1, 122.2, 120.2, 113.1, 52.2, 38.4, 35.0, 34.0, 32.0, 26.7. ES-MS(+) m/z 380, 381 (MH^+).

General Procedure for the Preparation of 2-(2-Substituted-thiazol-4-yl)-3-cyclopentyl-1*H*-indole-6-carboxylic Acid Building Blocks 5−11. Bromomethyl ketone **14** (1 equiv) was dissolved in isopropanol or dioxane (5−10 mL per mmol of **14**), and a thiourea, acylthiourea, or thioamide (1.1−1.25 equiv) was added. The mixture was heated to 65−80 °C until reaction was complete as judged by HPLC analysis. Volatiles were removed under reduced pressure, and the residue was purified by flash chromatography or saponified directly using 5 N NaOH or LiOH hydrate in a 1:1 mixture of MeOH and THF at room temperature until complete. Following acidification of the reaction mixture with aqueous HCl, the desired indolecarboxylic acid was isolated by extraction with EtOAc, washed with water and brine, dried ($MgSO_4$) and volatiles were removed from the desired product. The crude carboxylic acid derivatives were isolated as amber solids and used directly for coupling with right-hand-side fragments **A**−**H** in the usual manner.

(*S*)-3-(9*H*-Fluoren-9-ylmethoxycarbonylamino)pyrrolidine-1,3-dicarboxylic Acid 1-*tert*-Butyl Ester, (*S*)-16. (S)-Cucurbitine **15** (0.267 g, 2.05 mmol) was dissolved in THF (15 mL), and 1 N NaOH (4.1 mL, 4.1 mmol) was added followed by Boc_2O (0.49 g, 2.26 mmol). The reaction mixture was stirred overnight at room temperature, and Fmoc-ONSu (1.038 g, 3.08 mmol) was added. After being stirred at room temperature for an additional 20 h, the reaction mixture was acidified with 1 N HCl and extracted with EtOAc. The extract was washed with brine, dried ($MgSO_4$), and concentrated under reduced pressure to give crude material (1.36 g) that was used as such in the next step.

(*S*)-3-(9*H*-Fluoren-9-ylmethoxycarbonylamino)-1-methylpyrrolidine-3-carboxylic Acid, (*S*)-17. The crude material from above (1.36 g) was dissolved in CH_2Cl_2 (4 mL), and TFA (4 mL) was added. The solution was stirred for 45 min at room temperature, and then volatiles were removed under reduced pressure. The residue was dissolved in EtOH (20 mL), and AcOH (1.06 mL, 18.5 mmol) was added followed by 37% aqueous formaldehyde (1 mL, 12.3 mmol) and sodium cyanoborohydride (0.39 g, 6.1 mmol). The reaction mixture was stirred for 1 h at room temperature. (*S*)-Cucurbitine derivative **17** was isolated as a white solid TFA salt by semipreparative HPLC using aqueous TFA−acetonitrile gradients (~400 mg) and was used as such for the next step.

(*E*)-3-{4-[((*S*)-3-Amino-1-methylpyrrolidine-3-carbonyl)-amino]phenyl}acrylic Acid Ethyl Ester, Fragment A Ethyl Ester. TFA salt (*S*)-**17** (107 mg, 0.22 mmol) and ethyl 4-aminocinnamate (54 mg, 0.28 mmol) were dissolved in DMF (2.5 mL). HATU (128 mg, 0.34 mmol) and HOAt (46 mg, 0.34 mmol) were then added, followed by 2,4,6-collidine (89 μL, 0.67 mmol). The reaction mixture was stirred at 50 °C for 2.5 h after which additional HATU was added to complete the conversion as monitored by HPLC analysis. After completion, the reaction mixture was cooled to room temperature, acidified with a few drops of AcOH and the mixture purified by semipreparative HPLC to provide fragment **A** as a yellowish TFA salt (91 mg, 62% yield).

(*E*)-3-(4-Aminophenyl)-2-methylacrylic Acid, Methyl Ester (20). α-Methyl-4-nitrocinnamic acid **19** (53 mg, 0.25 mmol) was dissolved in EtOAc and MeOH, and a solution of CH_2N_2 in Et_2O was added until a persistent yellow color was observed. A couple of drops of AcOH were added to destroy the excess CH_2N_2. The mixture was diluted with EtOAc, and the organic layer was washed with H_2O, aqueous NaOH (1 N), and brine, dried over anhydrous $MgSO_4$, and concentrated to dryness. The residue was redissolved in EtOH (2 mL). $SnCl_2{\cdot}2H_2O$ (289 mg, 1.28 mmol) was added, and the reaction mixture was heated to reflux for 1 h. The mixture was cooled to room temperature, diluted with EtOAc, and quenched by the addition of aqueous, saturated $NaHCO_3$. The organic layer was separated, washed with brine, dried over anhydrous $MgSO_4$, and concentrated to dryness to give the title compound (40 mg) as a yellow solid. ES^+ MS m/z: 206.0 $(M + H)^+$. ES^- MS m/z: 204.0 $(M - H)^-$.

Biological Testing. Inhibition of HCV polymerase activity in a biochemical assay was performed using an NS5BΔ21 construct as previously described.[25a] Reported values are the average of duplicate measurements. EC_{50} determinations in the cell-based 1b replicon assay were performed in duplicate using RT-PCR for RNA quantification as described elsewhere.[34]

Pharmacokinetic Experiments. All protocols involving animal experimentation were reviewed and approved by the respective Animal Care and Use Committee of each test facility. In-life procedures were in compliance with the Guide for the Care and Use of Laboratory Animals from the Canadian Council of Animal Care. All rat PK studies were performed at Boehringer Ingelheim (Canada) Ltd. PK studies in dogs and monkeys were performed at LAB Pre-Clinical Research International Inc., Laval, Quebec, Canada. All chemicals used were reagent grade or better.

Animals were starved overnight and then dosed either at the iv dose of 2 mg/kg (in 70% PEG400) or at the oral dose of 10 mg/kg (in a suspension containing 0.3% Tween-80 and 0.5% Methocel). In the cassette screen experiments, each "cassette" containing four compounds at 4 mg/kg for each compound was dosed to two rats. Blood samples collected from all time points were placed on ice and then centrifuged at 4 °C. The plasma was separated and stored frozen at approximately −20 °C until analysis.

Plasma samples were extracted by solid phase extraction using Waters Oasis HLB 60 mg cartridges. Samples were injected on an HPLC system (Waters Alliance 2690 or 600E system controller with 717+ autosampler and 625 pump) using a Waters XTerra C8 column (2.1 mm × 100 mm, 5 μm). Detection was performed using UV diode array (Waters PDA 996) between 200 and 400 nm with quantitative determination made by peak height at the wavelength representing the best signal-to-noise ratio. Calibration standards were prepared in blank plasma. The calibration curve was linear to cover the time−concentration curve with a r^2 > 0.99 and a limit of quantification (LOQ) at 6 ng/mL. The temporal profiles of drug concentrations in plasma were analyzed by noncompartmental methods using WinNonlin (version 3.1; Scientific Consulting, Inc., Cary, NC).

■ ASSOCIATED CONTENT

Supporting Information

The enzymatic and 1b replicon potencies of all compounds displayed in graphical format in Figures 4 and 5, human and rat liver microsome stability, Caco-2 permeability and plasma concentrations following oral dosing in rats, mass spectral and HPLC homogeneity data, and ^{1}H NMR spectra for all inhibitors. This material is available free of charge via the Internet at http://pubs.acs.org.

AUTHOR INFORMATION

Corresponding Author

*Phone: (450) 682 4640. Fax: (450) 682 8434. E-mail: pierre.beaulieu@boehringer-ingelheim.com.

Notes

The authors declare no competing financial interest.

ACKNOWLEDGMENTS

We thank the following colleagues from Boehringer Ingelheim (Canada) Ltd. who participated in generating the data presented in this paper and contributed to the discovery of BILB 1941: Nathalie Dansereau, Lisette Lagacée, Martin Marquis, and Charles Pellerin for IC_{50} and EC_{50} determinations; Josie De Marte, Francine Liard, Hélène Montpetit, and Christine Zouki for ADME-PK support; Norman Aubry, Colette Boucher, Graham McGibbon, and Serge Valois for analytical support; Paul C. Anderson and Daniel Lamarre for helpful discussions.

ABBREVIATIONS USED

HCV, hepatitis C virus; DAA, direct acting antiviral; HCC, hepatocellular carcinoma; PegIFN, pegylated interferon; RBV, ribavirin; gt1, genotype 1; SVR, sustained viral response; SoC, standard of care; RdRp, RNA-dependent RNA polymerase; ADME, absorption, distribution, metabolism, excretion; PK, pharmacokinetics; SAR, structure−activity relationship; HLM, human liver microsomes; RLM, rat liver microsome; BSA, bovine serum albumin; CYP, cytochrome P-450; iv, intravenous; TFA, trifluoroacetic acid; TBME, *tert*-butyl methyl ether; THF, tetrahydrofuran; DMF, *N*,*N*-dimethylformamide; HATU, *O*-(7-azabenzotriazol-1-yl)-*N*,*N*,*N*′,*N*′-tetramethyluronium hexafluorophosphate; HOAt, 1-hydroxy-7-azabenzotriazole

REFERENCES

(1) Choo, Q.-L.; Kuo, G.; Weiner, A. J.; Overby, L .R.; Bradley, D. W.; Houghton, M. Isolation of a cDNA clone derived from a blood-borne non-A, non-B viral hepatitis genome. *Science* **1989**, *244*, 359−362.

(2) Lavanchy, D. Evolving epidemiology of hepatitis C virus. *Clin. Microbiol. Infect.* **2011**, *17*, 107−115.

(3) Simmonds, P. Genetic diversity and evolution of hepatitis C virus—15 years on. *J. Gen. Virol.* **2004**, *85*, 3173−3188.

(4) (a) Wise, M.; Bialek, S.; Finelli, L.; Bell, B.; Sorvillo, F. Changing trends in hepatitis C-related mortality in the United States, 1995−2004. *Hepatology* **2008**, *47*, 1128−1135. (b) Davis, G. L.; Albright, J. E.; Cook, S. F.; Rosenberg, D. M. Projecting future complications of chronic hepatitis C in the United States. *Liver Transplant.* **2003**, *9*, 331−338.

(5) (a) Bosetti, C.; Levi, F.; Lucchini, F.; Zatonski, W. A.; Negri, E.; La Vecchia, C. Worldwide mortality from cirrhosis: an update to 2002. *J. Hepatol.* **2007**, *46*, 827−839. (b) Wise, M.; Bialek, S.; Finelli, L.; Bell, B. P.; Sorvillo, F. Changing trends in hepatitis C-related mortality in the United States. *Hepatology* **2008**, *47*, 1128−1135. (c) Davila, J. A.; Morgan, R. O.; Shaib, Y.; McGlynn, K. A.; El-Serag, H. B. Hepatitis C infection and the increasing incidence of hepatocellular carcinoma: a population-based study. *Gastroenterology* **2004**, *127*, 1372−1380.

(6) (a) Fried, M. W.; Shiffman, M. L.; Reddy, K. R.; Smith, C.; Marinos, G.; Gonçales, F. L., Jr.; Haüssinger, D.; Diago, M.; Carosi, G.; Dhumeaux, D.; Craxi, A.; Lin, A.; Hoffman, J.; Yu, J. Peginterferon alfa-2a plus ribavirin for chronic hepatitis C virus infection. *N. Engl. J. Med.* **2002**, *347*, 975−982. (b) Zeuzem, S.; Berg, T.; Moeller, B.; Hinrichsen, H.; Mauss, S.; Wedemeyer, H.; Sarrazin, C.; Hueppe, D.; Zehnter, E.; Manns, M. P. Expert opinion on the treatment of patients with chronic hepatitis C. *J. Viral Hepatitis* **2009**, *16*, 75−90.

(7) (a) National Institutes of Health consensus development conference statement: management of hepatitis C 2002 (June 10−12, 2002). *Gastroenterology* **2002**, *123*, 2082−2099. (b) Manns, M. P.; Foster, G. R.; Rockstroh, J. K.; Zeuzem, S.; Zoulim, F.; Houghton, M. The way forward in HCV treatment—finding the right path. *Nat. Rev. Drug Discovery* **2007**, *6*, 991−1000. (c) Björnsson, E.; Verbaan, H.; Oksanen, A.; Frydén, A.; Johansson, J.; Friberg, S.; Dalgård, O.; Kalaitzakis, E. Health-related quality of life in patients with different stages of liver disease induced by hepatitis C. *Scand. J. Gastroenterol.* **2009**, *44*, 878−887.

(8) Lohmann, V.; Körner, F.; Koch, J. O.; Herian, U.; Theilmann, L.; Bartenschlager, R. Replication of subgenomic hepatitis C virus RNAs in a hepatoma cell line. *Science* **1999**, *285*, 110−113.

(9) (a) Wakita, T.; Pietschmann, T.; Kato, T.; Date, T.; Miyamoto, M.; Zhao, Z.; Murthy, K.; Habermann, A.; Kräusslich, H.-G.; Mizokami, M.; Bartenschlager, R.; Liang, T. G. Production of infectious hepatitis C virus in tissue culture from a cloned viral genome. *Nat. Med.* **2005**, *11*, 791−796. (b) Lindenbach, B. D.; Evans, M. J.; Syder, A. J.; Wölk, B.; Tellinghuisen, T. L.; Liu, C. C.; Maruyama, T.; Hynes, R. O.; Burton, D. R.; McKeating, J. A.; Rice, C. M. *Science* **2005**, *309*, 623−626.

(10) Tan, S.-L.; He, Y. *Hepatitis C: Antiviral Drug Discovery and Development*; Caister Academic Press: Norwich, U.K., 2011.

(11) Lindenbach, B. D.; Rice, C. M. Unraveling hepatitis C virus replication from genome to function. *Nature* **2005**, *436*, 933−938.

(12) (a) Hinrichsen, H.; Benhamou, Y.; Wedemeyer, H.; Reiser, M.; Sentjens, R. E.; Calleja, J. L.; Forns, X.; Erhardt, A.; Cröenlein, J.; Chaves, R.; Yong, C. −L.; Nehmiz, G.; Steinmann, G. G. Short-term antiviral efficacy of BILN 2061, a HCV serine protease inhibitor, in hepatitis C genotype 1 patients. *Gastroenterology* **2004**, *127*, 1347−1355. (b) Lamarre, D.; Anderson, P. C.; Bailey, M.; Beaulieu, P.; Bolger, G.; Bonneau, P.; Bös, M.; Cameron, D. R.; Cartier, M.; Cordingley, M. G.; Faucher, A.-M.; Goudreau, N.; Kawai, S. H.; Kukolj, G.; Lagacé, L.; LaPlante, S. R.; Narjes, H.; Poupart, M.-A.; Rancourt, J.; Sentjens, R. E.; St George, R.; Simoneau, B.; Steinmann, G.; Thibeault, D.; Tsantrizos, Y.; Weldon, S. M.; Yong, C.-L.; Llinàs-Brunet, M. An NS3 protease inhibitor with antiviral effects in humans infected with hepatitis C virus. *Nature* **2003**, *426*, 186−189.

(13) (a) Gentile, I.; Carleo, M. A.; Borgia, F.; Castaldo, G.; Borgia, G. The efficacy and safety of telaprevir: a new protease inhibitor against hepatitis C virus. *Expert Opin. Invest. Drugs* **2010**, *19*, 151−159. (b) Kwong, D. A.; Kauffman, R. S.; Mueller, P. Discovery and development of telaprevir: an NS3-4A protease inhibitor for treating genotype 1 chronic hepatitis C virus. *Nat. Biotechnol.* **2011**, *29*, 993−1003. (c) Berman, K.; Kwo, P. Y. Boceprevir, an NS3 protease inhibitor of HCV. *Clin. Liver Dis.* **2009**, *13*, 429−439. (d) Asselah, T.; Marcellin, P. New direct-acting antivirals combination for the treatment of chronic hepatitis C. *Liver Int.* **2011**, *31*, 68−77.

(14) (a) Sarrazin, C.; Zeuzem, S. Resistance to direct antiviral agents in patients with hepatitis C virus infection. *Gastroenterology* **2010**, *138*, 447−462. (b) Gaudieri, S.; Rauch, A.; Pfafferott, K.; Barnes, E.; Cheng, W.; McCaughan, G.; Shackel, N.; Jeffrey, G. P.; Mollison, L.; Baker, R.; Furrer, H.; Günthard, H. F.; Freitas, E.; Humphreys, I.; Klenerman, P.; Mallal, S.; James, I.; Roberts, S.; Nolan, D.; Lucas, M. Hepatitis C virus drug resistance and immune-driven adaptations: relevance to new antiviral therapy. *Hepatology* **2009**, *49*, 1069−1082.

(15) (a) White, P. W.; Llinàs-Brunet, M.; Amad, M.; Bethell, R. C.; Bolger, G.; Cordingley, M. G.; Duan, J.; Garneau, M.; Lagacé, L.; Thibeault, D.; Kukolj, G. Preclinical characterization of BI 201335, a C-terminal carboxylic acid inhibitor of the hepatitis C virus NS3-NS4A protease. *Antimicrob. Agents Chemother.* **2010**, *54*, 4611−4618. (b) Lin, T.-I.; Lenz, O.; Fanning, G.; Verbinnen, T.; Delouvroy, F.; Scholliers, A.; Vermeiren, K.; Rosenquist, Å.; Edlund, M.; Samuelsson, B.; Vrang, L.; de Kock, H.; Wigerinck, P.; Raboisson, P.; Simmen, K. In vitro activity and preclinical profile of TMC435350, a potent hepatitis C virus protease inhibitor. *Antimicrob. Agents Chemother.* **2009**, *53*, 1377−1385.

(16) (a) Soriano, V. A new era for hepatitis C—new diagnostics tools and new weapons. *ACS Med. Chem. Lett.* **2012**, *3*, 440−441. (b) Gane,

D. Future hepatitis C virus treatment: interferon-sparing combinations. *Liver Int.* **2011**, *31*, 62−67. (c) Cordek, D. G.; Bechtel, J. T.; Maynard, A. T.; Kazmierski, W. M.; Cameron, C. E. Targeting the NS5A protein on HCV: an emerging option. *Drugs Future* **2011**, *36*, 691−711. (d) Sulkowski, M.; Gardiner, D.; Lawitz, E.; Hinestrosa, F.; Nelson, D.; Thuluvath, P.; Rodriguez-Torres, M.; Lok, A.; Schwartz, H.; Reddy, K. R.; Eley, T.; Wind-Rotolo, M.; Huang, J.-P.; Gao, M.; McPhee, F.; Hindes, R.; Symonds, B.; Pasquinelli, C.; Grasela, D. Potent viral suppression with all-oral combination of daclatasvir (NS5A inhibitor) and GS-7977 (NS5B inhibitor), ± ribavirin, in treatment-naive patients with chronic HCV GT1, 2, or 3. *J. Hepatol.* **2012**, *56* (Suppl. 2), S560.

(17) (a) Kolykhalov, A. A.; Mihalik, K.; Feinstone, S. M.; Rice, C. M. Hepatitis C virus-encoded enzymatic activities and conserved RNA elements in the 3′-nontranslated region are essential for virus replication in vivo. *J. Virol.* **2000**, *74*, 2046−2051. (b) Chinnaswamy, S.; Yarbrough, I.; Palaninathan, S.; Kumar, C. T. R.; Vijayaraghavan, V.; Demeler, B.; Lemon, S. M.; Sacchettini, J. C.; Kao, C. C. A locking mechanism regulates RNA synthesis and host protein interaction by the hepatitis C virus polymerase. *J. Biol. Chem.* **2008**, *283*, 20535−20546. (c) Harrus, D.; Ahmed-El-Sayed, N.; Simister, P. C.; Miller, S.; Triconnet, M.; Hagedorn, C. H.; Mahias, K.; Rey, F. A.; Astier-Gin, T.; Bressanelli, S. Further insights into the roles of GTP and the C-terminus of the hepatitis C virus polymerase in the initiation of RNA synthesis. *J. Biol. Chem.* **2010**, *285*, 32906−32918.

(18) Bressanelli, S.; Tomei, L.; Roussel, A.; Incitti, I.; Vitale, R. L.; Mathieu, M.; De Francesco, R.; Rey, F. A. Crystal structure of the RNA-dependent RNA polymerase of hepatitis C virus. *Proc. Natl. Acad. Sci. U.S.A.* **1999**, *96*, 13034−13039.

(19) For reviews on NS5B inhibitors see, for example, the following: (a) Beaulieu, P. L. Recent advances in the development of NS5B polymerase inhibitors for the treatment of hepatitis C virus infection. *Expert Opin. Ther. Pat.* **2009**, *19*, 145−164. (b) Watkins, W. J.; Ray, A. S.; Chong, L. S. HCV NS5B polymerase inhibitors. *Cur. Opin. Drug Discovery Dev.* **2010**, *13*, 441−465. (c) Sofia, M. J.; Chang, W.; Furman, P. A.; Mosley, R. T.; Ross, B. S. Nucleoside, nucleotide, and non-nucleoside inhibitors of hepatitis C virus NS5B RNA-dependent RNA-polymerase. *J. Med. Chem.* **2012**, *55*, 2532−2531.

(20) (a) Brown, N. A. Progress towards improving antiviral therapy for hepatitis C virus polymerase inhibitors. Part 1: nucleoside analogues. *Expert Opin. Invest. Drugs* **2009**, *18*, 709−725. (b) Furman, P. A.; Lam, A. M.; Murakami, E. Nucleoside analog inhibitors of hepatitis C virus replication: recent advances, challenges and trends. *Future Med. Chem.* **2009**, *1*, 1429−1452. (c) Sofia, M. J. Nucleotide prodrugs for HCV therapy. *Antiviral Chem. Chemother.* **2011**, *22*, 23−49.

(21) (a) Le Pogam, S.; Jiang, W.-R.; Leveque, V.; Rajyaguru, S.; Ma, H.; Kang, H.; Jiang, S.; Singer, M.; Ali, S.; Klumpp, K.; Smith, D.; Symons, J.; Cammack, N.; Nájera, I. In vitro selected Con1 subgenomic replicons resistant to 2′-*C*-methyl-cytidine or to R1479 show lack of cross-resistance. *Virology* **2006**, *351*, 340−348. (b) McCown, M. F.; Rajyaguru, S.; Le Pogam, S.; Ali, S.; Jiang, W.-R.; Kang, H.; Symons, J.; Cammack, N.; Nájera, I. The hepatitis C virus replicon presents a higher barrier to resistance to nucleoside analogs than to non-nucleoside polymerase or protease inhibitors. *Antimicrob. Agents Chemother.* **2008**, *52*, 1604−1612. (c) Le Pogam, S.; Seshaadri, A.; Ewing, A.; Kang, H.; Kosaka, A.; Yan, J.-M.; Berrey, M.; Symonds, B.; DeLaRosa, A.; Cammack, N.; Nájera, I. RG1728 alone or in combination with pegylated interferon-α2a and ribavirin prevents hepatitis C virus (HCV) replication and selection of resistant variants in HCV-infected patients. *J. Infect. Dis.* **2010**, *202*, 1510−1519. (d) Gane, E. J.; Roberts, S. K.; Stedman, C. A. M.; Angus, Q. W.; Ritchie, B.; Elston, R.; Ipe, D.; Morcos, P. N.; Baher, L.; Nájera, I.; Chu, T.; Lopatin, U.; Berrey, M. M.; Bradford, W.; Laughlin, M.; Shulman, N. S.; Smith, P. F. Oral combination therapy with a nucleoside polymerase inhibitor (RG7128) and danoprevir for chronic hepatitis C genotype 1 infection (INFORM-1): a randomized, double-blind, placebo-controlled, dose-escalation trial. *Lancet* **2010**, *376*, 1467−1475.

(22) (a) Chinnaswamy, S.; Murali, A.; Li, P.; Fujisaki, K.; Kao, C. C. Regulation of de novo-initiated RNA synthesis in hepatitis C virus RNA-dependent RNA polymerase by intermolecular interactions. *J. Virol.* **2010**, *84*, 5923−5935. (b) Rigat, K.; Wang, Y.; Hudyma, T. W.; Ding, M.; Zheng, X.; Gentles, R. G.; Beno, B. R.; Gao, M.; Roberts, S. B. Ligand-induced changes in hepatitis C virus NS5B polymerase structure. *Antiviral Res.* **2010**, *88*, 197−206.

(23) Li, H.; Shi, S. T. Non-nucleoside inhibitors of hepatitis C virus polymerase: current progress and future challenges. *Future Med. Chem.* **2010**, *2*, 121−141.

(24) (a) Sofia, M. J.; Furman, P. A.; Symonds, W. T. 2′-*F*-2′-*C*-Methyl Nucleosides and Nucleotides for the Treatment of Hepatitis C Virus: From Discovery to the Clinic. In *Accounts in Drug Discovery: Case Studies in Medicinal Chemistry*; Barrish, J. C., Carter, P. H., Cheng, P. T. W., Zhaler, R., Eds.; Royal Society of Chemistry: Cambridge, U.K., 2010; Vol. 4, pp 238−266. (b) Zhou, X. J.; Pietropaolo, K.; Chen, J.; Khan, S.; Sullivan-Bolyai, J.; Mayers, D. Safety and pharmacokinetics of IDX184, a liver-targeted nucleotide polymerase inhibitor of hepatitis C virus, in healthy subjects. *Antimicrob. Agents Chemother.* **2011**, *55*, 76−81. (c) Sofia, M. J.; Bao, D.; Chang, W.; Du, J.; Nagaratham, D.; Rachakonda, S.; Reddy, P. G.; Ross, B. S.; Wang, P.; Zhang, H.-R.; Bansal, S.; Espiritu, C.; Keilman, M.; Lam, A. M.; Steuer, H. M. M.; Niu, C.; Otto, M. J.; Furman, P. A. Discovery of a β-D-2′-deoxy-2′-α-fluoro-2′-β-*C*-methyluridine nucleotide prodrug (PSI-7977) for the treatment of hepatitis C virus. *J. Med. Chem.* **2010**, *53*, 7202−7218. (d) McGuigan, C.; Madela, K.; Aljarah, M.; Gilles, A.; Brancale, A.; Zonta, N.; Chamberlain, S.; Vernachio, J.; Hutchins, J.; Hall, A.; Ames, B.; Gorovits, E.; Ganguly, B.; Kolykhalov, A.; Wang, J.; Muhammad, J.; Patti, J. M.; Henson, G. Design, synthesis and evaluation of a novel double prodrug: INX-08189. A new clinical candidate for hepatitis C virus. *Bioorg. Med. Chem. Lett.* **2010**, *20*, 4850−4854. (e) Kadow, J. F.; Gentles, R.; Ding, M.; Bender, J.; Bergstrom, C.; Grant-Young, K.; Hewawasam, P.; Hudyma, T.; Martin, S.; Nickel, A.; Regueiro-Ren, A.; Tu, Y.; Yang, Z.; Yeung, K.-S.; Zheng, X.; Chen, B.-C.; Chao, S.; Sun, J.-H.; Li, J.; Mathur, A.; Smith, D.; Wu, D.-R.; Beno, B.; Hanumegowda, U.; Knipe, J.; Parker, D. D.; Zhuo, X.; Lemm, J.; Liu, M.; Pelosi, L.; Rigat, K.; Voss, S.; Wang, Y.; Wang, Y.-K.; Colonno, R.; Gao, M.; Roberts, S. B.; Meanwell, N. A. Discovery of BMS-791325, an Allosteric NS5B Replicase Inhibitor for the Treatment of Hepatitis C. Presented at the 243rd National Meeting of the American Chemical Society, San Diego, CA, March 25−29, 2012; MEDI-23. (f) Vendeville, S.; Lin, T.-I.; Hu, L.; Tahn, A.; MgGowan, D.; Cummings, M. D.; Amssoms, K.; Last, S.; Devogelaere, B.; Rouan, M.-C.; Vigen, L.; Berke, J. M.; Dehertogh, P.; Fransen, E.; Cleiren, E.; van der Heim, L.; Fanning, G.; Van Emeien, K.; Nyanguile, O.; Simmen, K.; Raboisson, P. Discovery of the Clinical Candidate TMC 647055, a Non-Nucleoside Inhibitor of the Hepatitis C Virus NS5B Polymerase. Presented at the 18th International Symposium on Hepatitis C Virus and Related Viruses, Seattle, WA, Sept 8−12, 2011; Abstract P1.33. (g) Rosario, M.; Chauret, N.; George, S.; Kieffer, T. L.; Koziel, M. J.; Nicolas, O.; Proulx, L. Therapies for Treating Hepatitis C Virus Infection. Patent WO 2011/094489, August 4, 2011. (h) Li, H.; Tatlock, J.; Linton, A.; Gonzalez, J.; Jewell, T.; Patel, L.; Ludlum, S.; Drowns, M.; Rahavendran, S. V.; Skor, H.; Hunter, R.; Shi, S. T.; Herlihy, K. J.; Parge, H.; Hickey, M.; Yu, X.; Chau, F.; Nonomiya, J.; Lewis, C. Discovery of (*R*)-6-cyclopentyl-6-(2-(2,6-diethylpyridin-4-yl)ethyl)-3-((5,7-dimethyl-[1,2,4]triazolo[1,5,*a*]-pyrimidin-2-yl)-methyl-4-hydroxy-5,6-dihydropyran-2-one (PF-00868554) as a potent and orally available hepatitis C virus polymerase inhibitor. *J. Med. Chem.* **2009**, *52*, 1255−1258. (i) Tran, C. V.; Ruebsam, F.; Murphy, D. E.; Dragovich, P.; Zhou, Y.; Chen, L.; Kuccera, D. 5,6-Dihydro-1*H*-pyridin-2-one compounds. Patent 7,939,524, May 10, 2011 (see also www.ama-assn.org/resources/doc/usan/lomibuvir.pdf).

(25) (a) McKercher, G.; Beaulieu, P. L.; Lamarre, D.; LaPlante, S.; Lefebvre, S.; Pellerin, C.; Thauvette, L.; Kukolj, G. Specific inhibitors of HCV polymerase identified using a NS5B with lower affinity for template/primer substrate. *Nucleic Acids Res.* **2004**, *32*, 422−431. (b) Beaulieu, P. L.; Bös, M.; Bousquet, Y.; Fazal, G.; Gauthier, J.; Gillard, J.; Goulet, S.; LaPlante, S.; Poupart, M.-A.; Lefebvre, S.;

McKercher, G.; Pellerin, C.; Austel, V.; Kukolj, G. Non-nucleoside inhibitors of the hepatitis C virus NS5B polymerase: discovery and preliminary SAR of benzimidazole derivatives. *Bioorg. Med. Chem. Lett.* **2004**, *14*, 119−124. (c) Beaulieu, P. L. Finger loop inhibitors of the HCV NS5B polymerase: discovery and prospects for new HCV therapy. *Cur. Opin. Drug Discovery Dev.* **2006**, *9*, 618−626. (d) Hirashima, S.; Suzuki, T.; Ishida, T.; Noji, S.; Yata, S.; Ando, I.; Komatsu, M.; Ikeda, S.; Hashimoto, H. Benzimidazole derivatives bearing substituted biphenyls as hepatitis C virus NS5B RNA-dependent RNA polymerase inhibitors: structure−activity relationship studies and identification of a potent and highly selective inhibitor JTK-109. *J. Med. Chem.* **2006**, *49*, 4721−4736. (e) Narjes, F.; Crescenzi, B.; Ferrara, M.; Habermann, J.; Colarusso, S.; del Rosario, M.; Ferreira, R.; Stansfield, I.; Mackay, A. C.; Conte, I.; Ercolani, C.; Zaramella, S.; Palumbi, M.-C.; Meuleman, P.; Leroux-Roels, G.; Guiliano, C.; Fiore, F.; Di Marco, S.; Baiocco, P.; Koch, U.; Migliaccio, G.; Altamura, S.; Laufer, R.; De Francesco, R.; Rowley, M. Discovery of (7*R*)-14-cyclohexyl-7-{[2-(dimethylamino)ethyl](methyl)amino}-7,8-dihydro-6*H*-indolo[1,2-*e*][1,5]benzoxazocine-1-carboxylic acid (MK-3281), a potent and orally bioavailable finger-loop inhibitor of the hepatitis C virus NS5B polymerase. *J. Med. Chem.* **2011**, *54*, 289−301. (f) Zheng, X.; Hudyma, T. W.; Martin, S. W.; Bergstrom, C.; Ding, M.; He, F.; Romine, J.; Poss, M. A.; Kadow, J. F.; Chang, C.-H.; Wan, J.; Witmer, M. R.; Morin, P.; Camac, D. M.; Sheriff, S.; Beno, B. R.; Rigat, K. L.; Wang, Y.-K.; Fridell, F.; Lemm, J.; Qiu, D.; Liu, M.; Voss, S.; Pelosi, L.; Roberts, S. B.; Gao, M.; Knipe, J.; Gentles, R. G. Syntheses and intitial evaluation of a series of indolo-fused heterocyclic inhibitors of the polymerase enzyme (NS5B) of the hepatitis C virus. *Bioorg. Med. Chem. Lett.* **2011**, *21*, 2925−2929.

(26) (a) Beaulieu, P. L.; Bös, M.; Bousquet, Y.; DeRoy, P.; Fazal, G.; Gauthier, J.; Gillard, J.; Goulet, S.; McKercher, G.; Poupart, M.-A.; Valois, S.; Kukolj, G. Non-nucleoside inhibitors of the hepatitis C virus NS5B polymerase: discovery of benzimidazole 5-carboxylic amide derivatives with low-nanomolar potency. *Bioorg. Med. Chem. Lett.* **2004**, *14*, 967−971. (b) Beaulieu, P. L.; Bousquet, Y.; Gauthier, J.; Gillard, J.; Marquis, M.; McKercher, G.; Pellerin, C.; Valois, S.; Kukolj, G. Non-nucleoside benzimidazole-based allosteric inhibitors of the hepatitis C virus NS5B polymerase: inhibition of subgenomic hepatitis C virus RNA replicons in Huh-7 cells. *J. Med. Chem.* **2004**, *47*, 6884−6892. (c) LaPlante, S. R.; Jakalian, A.; Aubry, N.; Bousquet, Y.; Ferland, J.-M.; Gillard, J.; Lefebvre, S.; Poirier, M.; Tsantrizos, Y. S.; Kukolj, G.; Beaulieu, P. L. Binding mode determination of benzimidazole inhibitors of the hepatitis C virus RNA polymerase by a structure and dynamics startegy. *Angew. Chem., Int. Ed.* **2004**, *43*, 4306−4311.

(27) (a) Goulet, S.; Poupart, M.-A.; Gillard, J.; Poirier, M.; Kukolj, G.; Beaulieu, P. L. Discovery of benzimidazole-diamide finger loop (thumb pocket 1) allosteric inhibitors of HCV NS5B polymerase: implementing parallel synthesis for rapid linker optimization. *Bioorg. Med. Chem. Lett.* **2010**, *20*, 196−200. (b) Kukolj, G.; McGibbon, G. A.; McKercher, G.; Marquis, M.; Lefèbvre, S.; Thauvette, L.; Gauthier, J.; Goulet, S.; Poupart, M.-A.; Beaulieu, P. L. Binding site characterization and resistance to a class of non-nucleoside inhibitors of the hepatitis C virus NS5B polymerase. *J. Biol. Chem.* **2005**, *280*, 39260−39267.

(28) (a) Beaulieu, P. L.; Gillard, J.; Jolicoeur, E.; Duan, J.; Garneau, M.; Kukolj, G.; Poupart, M.-A. From benzimidazole to indole 5-carboxamide thumb pocket 1 inhibitors of HCV NS5B polymerase. Part 1: Indole C-2 SAR and discovery of diamide derivatives with nanomolar potency in cell-based subgenomic replicons. *Bioorg. Med. Chem. Lett.* **2011**, *21*, 3658−3663. (b) Beaulieu, P. L.; Chabot, C.; Duan, J.; Garneau, M.; Gillard, J.; Jolicoeur, E.; Poirier, M.; Poupart, M.-A.; Stammers, T. A.; Kukolj, G.; Tsantrizos, Y. S. Indole 5-carboxamide thumb pocket 1 inhibitors of HCV NS5B polymerase with nanomolar potency in cell-based subgenomic replicons (part 2): central amino acid linker and right-hand-side SAR studies. *Bioorg. Med. Chem. Lett.* **2011**, *21*, 3664−3670. (c) LaPlante, S. R.; Gillard, J. R.; Jakalian, A.; Aubry, N.; Coulombe, R.; Brochu, C.; Tsantrizos, Y. S.; Poirier, M.; Kukolj, G.; Beaulieu, P. L. Importance of ligand bioactive conformation in the discovery of potent indole-diamide inhibitors of the hepatitis C virus NS5B. *J. Am. Chem. Soc.* **2010**, *132*, 15204−15212.

(29) Erhardt, A.; Deterding, K.; Benhamou, Y.; Reiser, M.; Forns, X.; Pol, S.; Calleja, J. L.; Ross, S.; Spangenberg, H. C.; Garcia-Samaniego, J.; Fuchs, M.; Enriquez, J.; Wiegand, J.; Stern, J.; Wu, K.; Kukolj, G.; Marquis, M.; Beaulieu, P.; Nehmiz, G.; Steffgen, J. Safety, pharmacokinetics and antiviral effect of BILB 1941, a novel hepatitis C virus RNA polymerase inhibitor, after 5 days oral treatment. *Antiviral Ther.* **2009**, *14*, 23−32.

(30) Beaulieu, P. L.; Gillard, J.; Bykowski, D.; Brochu, C.; Dansereau, N.; Duceppe, J.-S.; Haché, B.; Jakalian, A.; Lagacé, L.; LaPlante, S.; McKercher, G.; Moreau, E.; Perreault, S.; Stammers, T.; Thauvette, L.; Warrington, J.; Kukolj, G. Improved replicon cellular activity of non-nucleoside allosteric inhibitors of HCV NS5B polymerase: from benzimidazole to indole scaffolds. *Bioorg. Med. Chem. Lett.* **2006**, *16*, 4987−4993.

(31) (a) Vernin, G. In *Thiazole and Its Derivatives*; Metzger, J. V., Ed.; Wiley: New York, 1979; Part 1, Chapter 2.

(32) Paik, S.; Kwak, H. S.; Park, T. H. A facile synthesis of (−)-cucurbitine. *Bull. Korean Chem. Soc.* **2000**, *21*, 131−132.

(33) Rorrer, L. C.; Hopkins, S. D.; Connors, M. K.; Lee, D. W., III; Smith, M. V.; Rhodes, H. J.; Uffelman, E. S. A convenient new route to tetradentate and pentadentate macrocyclic tetraamide ligands. *Org. Lett.* **1999**, *1*, 1157−1159.

(34) Beaulieu, P. L.; Fazal, G.; Goulet, S.; Kukolj, G.; Poirier, M.; Tsantrizos, Y.; Jolicoeur, E.; Gillard, J.; Poupart, M.-A.; Rancourt, J. Patent WO 03/010141, 2003.